Article

Not peer-reviewed version

Comparison between the Regenerative and Therapeutic Impact of BM-MSCs and AD-MSCs Pre-treated with Melatonin on Liver Fibrosis

Ahmed Elzainy and Abir El Sadik *

Posted Date: 26 January 2024

doi: 10.20944/preprints202401.1871.v1

Keywords: Proliferation; inflammation; apoptosis; regeneration; therapy; liver

Article

Comparison between the Regenerative and Therapeutic Impact of BM-MSCs and AD-MSCs Pre-treated with Melatonin on Liver Fibrosis

Ahmed Elzainy [1] and Abir El Sadik [2,*]

[1] Department of Anatomy and Histology, College of Medicine, Qassim University, Buraydah 51452, Saudi Arabia; ahmedelzainy@qu.edu.sa
[2] Department of Anatomy and Embryology, College of Medicine, Cairo University, Egypt
* Correspondence: author: abeer.ouaida@kasralainy.edu.eg

Abstract: Background The distinctive feature of liver fibrosis is the progressive replacement of healthy hepatic cells by extracellular matrix protein, which is abundant in collagen I and III with impaired matrix remodelling. The activation of myofibroblastic cells enhances a fibrogenic response of complex interactions of hepatic stellate cells, fibroblasts and inflammatory cells to produce excessive deposition of extracellular protein matrix. This process is activated by multiple fibrogenic mediators and cytokines such as TNF-α and IL-1ß with decrease in the anti-fibrogenic factor NF-κß. Mesenchymal stem cells (MSCs) represent a promising therapy for liver fibrosis giving more advanced regenerative influence when cultured with extrinsic or intrinsic proliferative factors, cytokines, anti-oxidants, growth factors, and hormones such as Melatonin (MT). However, previous studies showed conflicted findings concerning the therapeutic effects of adipose (AD) and bone marrow (BM)-MSCs, therefore, the present work aimed to accomplish a comparative and comprehensive study investigating the impact of MT pre-treatment on the immunomodulatory, anti-inflammatory and anti-apoptotic effects of AD and BM-MSCs and to critically analyse whether MT pre-treated both AD-MSCs and BM-MSCs reveal equal or different therapeutic and regenerative potentials in CCl4-injured liver of experimental rat models. **Materials and methods** Six groups of experimental rats were used with ten rats in each group; group I (control group), group II (CCl4-treated group), group III (CCl4 and BM-MSCs treated group), group IV (CCl4 and MT pre-treated BM-MSCs group), group V (CCl4 and AD-MSCs treated group) and group VI (CCl4 and MT pre-treated AD-MSCs group). Liver function tests, gene expression of inflammatory, fibrogenic, apoptotic and proliferative factors were analysed. Histological and immunohistochemical changes were assessed. **Results** The present study compared the capability of AD and BM-MSCs, with and without the pre-treatment of MT, to reduce hepatic fibrosis. Both types of MSCs improved hepatocyte function by reducing the serum levels of (ALT), aspartate aminotransferase (AST), alkaline phosphatase (AKP), and total bilirubin (TBIL). In addition, the changes in the hepatocellular architecture including the hepatocytes, liver sinusoids, central veins, portal veins, biliary ducts and hepatic arteries showed decrease hepatocyte injury and cholestasis with reduction of inflammation, apoptosis and necrosis of the hepatic cells together with inhibition of liver tissue fibrosis. These results were augmented by the analysis of the expression of the anti-inflammatory cytokines TNFα and IL-1β, the anti-fibrogenic factor NF-κß, the apoptotic factor caspase-3 and the proliferative indicators antigen Ki-67 and proliferating cell nuclear antigen (PCNA). These findings were found statistically significant, with the best results in the rats received AD-MSCs pre-treated with MT, denoting better regenerative and therapeutic effects. **Conclusion** AD-MSCs, pre-treated with MT, are superior to BM-MSCs due to their better efficacy in improving hepatic fibrosis and promoting the therapeutic and regenerative capability of liver tissue. They represent a very significant tool for future stem cell use in tissue regeneration strategy for the treatment of liver diseases.

Keywords Proliferation; inflammation; apoptosis; regeneration; therapy; liver.

1. Introduction

Liver cirrhosis, the progression of liver fibrosis, currently is the eleventh most common cause of mortality worldwide and is continuously increasing (Asrani et al., 2019; Sepanlu et al., 2020; Liu et al., 2022). Liver fibrosis is considered one of the most serious health problems producing changes in

 doi:10.20944/preprints202401.1871.v1

the architecture and vasculature of some organs interrupting normal function (Karsdal et al., 2014; Suk and Kim, 2015). Liver fibrosis is a wound-healing procedure in which multiple consequences are induced including immune cell infiltration, myofibroblast activation, hepatocyte apoptosis and necrosis (Liu et al., 2022). Liver fibrosis is featured by the gradual replacement of functional hepatic cells by extracellular matrix protein, rich in collagen I and III, with impaired matrix remodelling (Lodder et al., 2015; Parola and Pinzani, 2018; Ma et al., 2022; Zhou et al., 2022). Excessive deposition of extracellular matrix is triggered by a fibrogenic response of complex interactions of matrix forming hepatic stellate cells, fibroblasts, and inflammatory cells. Hepatic stellate cells are allocated between the hepatocytes and sinusoid endothelial cells. They are activated by fibrogenic mediators and cytokines to differentiate into active myofibroblasts with the expression of pro-inflammatory mediators such as alpha-smooth muscle actin (α-SMA), tumor necrosis factor-alpha (TNF-α) and interleukin 1 beta (IL-1ß). (Yang and Seki, 2015; Hu et al., 2019; Masola et al., 2019; Mohammed et al., 2021; Kisseleva and Brenner, 2021). Numerous signalling pathways connected to inflammation, proliferation, and apoptosis can be triggered by TNF-α. TNFα has been associated with the pathogenesis of chronic liver inflammation with the activation of local hepatic stellate cells into fibrogenic myofibroblasts leading to liver fibrosis (Yang and Seki, 2015**)**. Consequently, control of hepatic stellate cell activation could potentially elicit the anti-fibrotic process (Roehlen et al., 2020). Therefore, extracellular matrix degradation and remodelling by blocking the myofibroblast signalling are crucial in reversing liver fibrosis and limiting its progression to cirrhosis. One significant and early mediator of fibrosis is IL-1β. It is induced within one hour of the pro-fibrotic procedure. It mediates the extracellular matrix degradation causing the hepatic sinusoids to collapse by inducing matrix metalloproteinase-9 (MMP-9) expression (Petrasek et al., 2012). Furthermore, IL-1β boosts the ability of activated hepatic stellate cells to survive (Pradere et al., 2013). The transcription and anti-fibrogenic element nuclear factor kappa β (NF-κß) is the principal regulator of inflammation and cell necrosis. Its normal activity in hepatocytes is to protect against liver fibrosis by inhibiting hepatocyte death. At the same time, decreased levels of NF-κß increased hepatocellular injury and fibrosis. NF-κß moderates hepatic fibrogenesis principally by controlling three different mechanisms. It regulates the first trigger of fibrogenic response which is hepatocyte injury. It reduces the inflammatory signals produced in macrophages and other inflammatory cells, and it controls the fibrogenic responses in hepatocyte stellate cells (Luedde and Schwabe, 2011). Therefore, regulation of the pro-inflammatory moderators; TNFα, IL-1β and increase the expression of anti-fibrogenic factor; NF-κß are crucial for the therapy and regeneration of the injured hepatocytes.

Mesenchymal stem cells (MSCs) represent a potential therapeutic strategy for liver fibrosis (Zhang et al., 2018; Kao et al., 2020; Shi et al., 2021; Xie et al., 2021). They are the most broadly applied type of stem cells obtained from multiple sources such as bone marrow, adipose tissue, umbilical cord, liver tissue, menstrual blood and placenta (Pelekanos et al., 2016; Huang et al., 2019; Shu et al., 2020; Varkouhi et al., 2021). The regenerative potential of MSCs was attributed to their highly proliferative, multipotent and differentiation capacity to replace damaged cells. However, it is currently believed that their paracrine action is responsible for the production of bioactive factors stimulating the subject's own progenitor cells' maturation and proliferation in addition to the release of immunoregulatory mediators that modulate the cascade of inflammation (El Sadik et al., 2015; Caplan, 2017; Liu et al., 2022). Therefore, the therapeutic effects of MSCs, in liver fibrosis, were suggested to be predisposed by their secretion of these factors rather than their ability to transform into hepatocytes that replace the damaged parenchymal cells (Zhou et al., 2019). Injured hepatocytes undergo apoptosis and necrosis influenced by multiple stimulators and signal pathways including transcription factors, inflammatory cytokines, chemokines, kinases, apoptotic mediators, growth factors, and oxidative stress products (Pellicoro et al., 2014; Forman, 2016). Bone marrow (BM)-MSCs could improve liver fibrosis in cirrhotic rat models (Jang et al., 2014). The authors reported a significant decrease in the collagen proportionate area and the downregulation of the TGF-B1/Smad signalling pathway. In addition, liver function was improved, fibrosis progression and hepatocyte necrosis were diminished. On the other hand, adipose tissue (AD)-MSCs have been proposed for cell-based therapy as a substitute for BM-MSCs. As a source of multipotent stem cells, AD-MSCs can be

 doi:10.20944/preprints202401.1871.v1

more easily isolated. They proliferate into larger numbers and continue to proliferate for 21 days more than BM-MSCs. AD-MSCs were found to yield more stem cells than BM-MSCs and differentiate in vitro and in vivo into hepatocytes (Tsuji et al., 2014). Moreover, BM-MSCs revealed more early senescence during expansion than AD-MSCs (Dmitrieva et al., 2012; Muthu et al., 2023). However, Hao, et al. (2017) reported that AD and BM-MSCs had similar effects in reducing liver fibrosis and preventing the activation and proliferation of hepatic stellate cells and enhancing their apoptosis. Both AD and BM-MSCs are influenced by extrinsic and intrinsic signalling factors such as cytokines, anti-oxidants, growth factors, extracellular matrix, enzymes and hormones. An example of these hormones is Melatonin (MT) which plays an important role in the regulation of cell proliferation. It has anti-inflammatory and anti-oxidant activities (Zhang et al., 2017). Recent studies determined that MT enhances the therapeutic effects of MSCs by promoting their self-renewal capability and reducing the inflammatory modulators expression (Li et al., 2019). Zhou, et al. (2015) detected that MT could prevent the replicative senescence of AD-MSCs. The maintenance of the biological activities of MSCs is controlled by complex mechanisms including intracellular and extracellular signalling pathways and the presence of potential immunomodulatory mediators in a favorable microenvironment. Therefore, the present work aimed to accomplish a comparative and comprehensive study investigating whether MT pre-treatment could improve the immunomodulatory, anti-inflammatory and anti-apoptotic effects of AD and BM-MSCs with the analysis of the expression of the anti-inflammatory cytokines TNFα and IL-1β, the anti-fibrogenic factor NF-ĸß, the apoptotic factor caspase-3 and the proliferative indicators antigen kiel 67 (Ki-67) and proliferating cell nuclear antigen (PCNA). Furthermore, different studies revealed conflicted findings comparing the therapeutic effects of AD and BM-MSCs, therefore, another aim of the current study is to critically analyse whether MT pre-treated both AD-MSCs and BM-MSCs reveal equal or different therapeutic and regenerative influence on apoptosis, inflammation and fibrosis in CCl4-injured liver of experimental rat models.

2. Materials and Methods

2.1. Isolation, Propagation and Identification of MSCs

Fluorescent-labeled BM and AD-MSCs were obtained from the Biochemistry and Molecular Biology Unit, Faculty of Medicine, Cairo University. Bone marrow was collected by flushing the femurs and tibiae of 6-week-old male rats with Dulbecco's modified Eagle's medium (DMEM, Sigma, USA, D5796) supplemented with 10% fetal bovine serum (Sigma, USA, F6178). The cells were layered in sterile conical tubes in a ratio of 2:1 over Ficoll-Hypaque (Sigma, USA, F8016) and then centrifuged. Isolated nucleated cells were resuspended in a complete culture medium supplemented with 1% penicillin-streptomycin (Sigma, USA, P4333). Cells were incubated at 37°C in 5% humidified CO2 for fourteen days as a primary culture with complete media replacement every four days. After the development of large colonies, at 80% confluence, the cultures were washed twice with phosphate buffer saline (PBS) (Sigma, USA, P5493). The cells were trypsinized with 0.25% trypsin (Sigma, USA, T1426) in 1ml Ethylene Diamine Tetra Acetate (EDTA) (Sigma, USA, E6758) for 5 minutes at 37°C. The cultures were centrifuged at 2400 rpm for 20 minutes. The cell pellets were suspended with serum-supplemented medium and then incubated in 25cm^2 culture flasks to form the first passage cultures (El Sadik et al., 2015; Abdelhafez et al., 2021). Adipose tissue was taken from the abdomen of Sprague Dawley albino rats after their sacrifice. Extracellular matrix was digested with 0.075% type I collagenase (37°C and 5% CO2 for 30min) and centrifuged at 500 g for 5min. The pellet was cultured in high glucose Dulbecco's modified Eagle's medium (DMEM, Sigma, USA, D5796) with 10% fetal bovine serum (Sigma, USA, F6178), 2mML glutamine, penicillin, and streptomycin (Invitrogen) and incubated 37°C in 5% humidified CO2. Non-adherent cells were removed after 48 hours and fresh media were added. When adherent cells were confluent, they were trypsinized, harvested, and expanded. All the experiments were performed using AD-MSCs at passage 3 (El Aasar et al., 2021). Identification of MSCs was determined by their morphology, adherence, detection

 doi:10.20944/preprints202401.1871.v1

of the surface markers of MSCs being positive for CD 34, 45, 90 and 105 and their power to differentiate into osteocytes and chondrocytes (Ode et al., 2011).

2.2. MT Pre-Treatment of MSCs

1ml of MT (Sigma-Aldrich Chemical Company, St. Louis, MO, USA) was added to 40ml of ethyl alcohol. The mixture was shaken for 2 minutes then 960 ml of saline were added to the mixture. MSCs were subjected to a 24-hours pre-treatment with 5 µL of MT equivalent to 1ml of the mixture. Complete removal of the hormone from cell suspension was confirmed by washing it three times with Phosphate Buffer Saline (PBS) (Sigma, USA) (Shuai et al., 2016; El Aasar et al., 2021).

2.3. Experimental Animals

A total of sixty adult male Sprague Dawley albino rats, weighing 150-200 grams, were used in the present study. Rats were maintained according to the standard guidelines of the Institutional Animal Care and Use Committee and after Institutional Review Board approval. The experiment proposal was approved by the Committee of Research Ethics, Deanship of Scientific Research, Qassim University; approval number 23-20-11. Rats were allowed to acclimatize for two weeks before the experiment, housed in cages under normal light/dark periods and fed a standard food and water *ad libitum*.

2.4. Experimental Design

The experimental rats were divided into the following groups:

Group I (Control, n=10): The rats received subcutaneous injections of 1ml saline twice weekly for 8 weeks and a single intravenous injection of 0.5ml PBS into the tail vein.

Group II (CCl4 group, n=10): The rats received subcutaneous injections of 1 ml/kg body weight CCl4 (Sigma-Aldrich Chemical Company, St Louis, Missouri, USA) at a ratio of 1:1 with corn oil twice weekly for 8 weeks to induce liver fibrosis (Wei et al., 2004).

Group III (CCl4 and BM-MSCs, n=10): Induction of fibrosis was performed as in group II. The rats received a single intravenous injection of BM-MSCs ($1x10^6$) diluted in 0.5 ml of PBS into the tail vein at the beginning of week 5 (El Sadik et al., 2015).

Group IV (CCl4 and MT pre-treated BM-MSCs, n=10): Induction of fibrosis was performed as in group II. The rats received a single intravenous injection of MT pre-treated BM-MSCs ($1x10^6$) diluted in 0.5 ml of PBS into the tail vein at the beginning of week 5.

Group V (CCl4 and AD-MSCs, n=10): Induction of fibrosis was performed as in group II. The rats received a single intravenous injection of AD-MSCs ($1x10^6$) diluted in 0.5 ml of PBS into the tail vein at the beginning of week 5.

Group VI (CCl4 and MT pre-treated AD-MSCs, n=10): Induction of fibrosis was performed as in group II. The rats received a single intravenous injection of MT pre-treated AD-MSCs ($1x10^6$) diluted in 0.5 ml of PBS into the tail vein at the beginning of week 5.

At the end of week 8, blood samples were collected from the experimental rats by retro-orbital plexus technique using capillary glass tubes. The collected blood samples were analysed for the levels of serum alanine aminotransferase (ALT), aspartate aminotransferase (AST), alkaline phosphatase (AKP), and total bilirubin (TBIL). The rats were sacrificed by overdose of intraperitoneal pentobarbital; 40 mg/kg body weight. Then, the liver of each animal was dissected and excised. Half of each liver specimen of each experimental rat was fixed in 10% formaldehyde in PBS at 4°C and was processed for paraffin blocks and prepared for light microscopic study. The other half was prepared directly for gene expression study.

2.5. Detection of Studied Genes by Quantitative Real Time Polymerase Chain Reaction (QRT-PCR)

Samples from the specimens obtained from the liver of the experimental rats (0.2 mg) were homogenized in PBS, pH 7.4 using tissue Lyzer (Qiagen; Hilden, Germany). The homogenate was centrifuged at 8000 xg for 20 minutes, then the supernatant was used for total RNA extraction. Total

 doi:10.20944/preprints202401.1871.v1

RNA was extracted using the RNeasy Mini Kit; cat no: 217004 (Qiagen, Hilden, Germany) according to the manufacturer's protocol. cDNA was synthesized by reverse transcription reaction using QuantiTect Reverse Transcription Kit; cat no: 205311; (Qiagen, Hilden, Germany). The gene expression for tumor necrosis factor alpha (TNF-α), interleukin 1 beta (IL-1ß) and the nuclear factor kappa β (NF-κß) levels was amplified from cDNA using the QuantiTect SYBR Green PCR Kit cat no: 204141 (Qiagen, Germany) and the QuantiTect primer assays cat no: 249900 [(Rn_Tnfrsf1a_1_SG QuantiTect Primer Assay, ID QT00388346), (Rn_Il1b_1_SG QuantiTect Primer Assay, ID QT00181657) and (Rn_Nfkb2_1_SG; ID: QT00396823)]; respectively. The ACTB Primer sequence was used as housekeeper gene. All samples were analyzed using the 5 plex Rotor-Gene PCR Analyzer (Qiagen, Germany). The 2ΔΔCt method was conducted for the analysis of gene expression levels, using ACTB as an endogenous reference control for normalization purposes (Wagner et al., 2012; Abdelhafez et al., 2021).

2.6. Light Microscopic Study

The liver specimens were fixed in 10% formaldehyde solution, processed, embedded in paraffin blocks, and cut at 5 µm thickness sections. The sections were then deparaffinised in xylol solution and rehydrated in 100%, 95% and 70% alcohol then washed in distilled water. Sections were prepared for the following examinations:

2.6.1. Hematoxylin and Eosin (H&E) Stain

The liver sections were stained with hematoxylin for ten minutes, then stained in 1% aqueous eosin for three minutes. The sections were dehydrated in alcohol (70 %, 90% and 100%) and then cleared by xylene. The slides were removed from xylol, mounted in Canada balsam and put on the cover slip.

2.6.2. Masson's Trichrome Stain

The liver sections were stained in Weigert's iron hematoxylin solution for 10 minutes, rinsed in running tap water for 10 minutes and washed in distilled water. Then they were stained in Biebrich scarlet-acid fuchsin solution for 15 minutes, washed in distilled water and differentiated in phosphomolybdic-phosphotungestic acid solution for 10 minutes. Then the sections were transferred to aniline blue solution for 10 minutes, rinsed shortly in distilled water and differentiated in 1% acetic acid solution for 5 minutes then rewashed in distilled water. The sections were dehydrated very quickly through absolute ethyl alcohol, cleared in xylene and finally mounted in Canada balsam. Collagen fibres appeared blue (Chen et al., 2009).

2.6.3. Periodic Acid-Schiff (PAS) Staining

Periodic acid solution was made of one gram of periodic acid in 200 ml distilled water. Schiff's reagent was formed of one gm basic fuchsine dissolved in 200 ml of boiling distilled water. The solution was left to cool to 50 °C. Two grams of potassium metabisulfite were added while mixing. Two ml of concentrated HCl acid were added after the solution was allowed to cool to room temperature. Mixed two grams of activated charcoal were added and left overnight in the dark at room temperature. The sections were treated with periodic acid for five minutes then washed with distilled water and covered with Schiff's solution for 15 minutes. After washing with running tap water, the nuclei were stained with Harri's hematoxylin, differentiated in acid-alcohol and blued as usual. The sections were washed in water, rinsed in absolute alcohol, cleared in xylene and mounted as desired. The polysaccharides were homogenously stained in the hepatocytes (Bancroft and Cook, 1994; El Sadik et al., 2018).

2.6.4. Immunofluorescent Study for Ki-67

Liver tissue was fixed in 4% formaldehyde in PBS for 15 min at room temperature. The tissue sections were covered with ice-cold 100% methanol, incubated in methanol for 10 min at -20°C, rinsed

 doi:10.20944/preprints202401.1871.v1

in PBS for 5 min, and blocked in a blocking buffer for 60 min. The blocking solution was aspirated and the diluted primary antibody was applied; anti-Ki-67 Polyclonal Antibody (Invitrogen; ThermoFisher Scientific, Hilden; Germany Catalogue Number PA5-16785). The specimens were incubated in fluorochrome-conjugated secondary antibody diluted in an Antibody Dilution Buffer for 2 hours at room temperature in the dark (Goat anti-rabbit IgG (H+L) Alexa Flour 488 Invitrogen; ThermoFisher Scientific, Hilden; Germany Catalogue Number A-11034). Slides were covered with Prolong® Gold Antifade Reagent (#9071) or Prolong® Gold Antifade Reagent with DAPI (#8961). Microscopic examination using appropriate excitation wavelength was performed by LABOMED Fluorescence microscope LX400, cat no: 9126000; USA.

2.6.5. Immunohistochemical Reaction

The specimens were cut at 5 μm thickness and then collected on Poly-L-lysine coated slides. The sections were deparaffinized in two changes of xylene and rehydrated through graded washes of ethanol in water, and finally rinsed in pure water. They were treated with 0.9% hydrogen peroxide in absolute methanol for 10 min. Antigen retrieval was achieved by heating the sections in 10 mm sodium citrate buffer, in a water bath at 95°C for 30 min. The sections were rinsed twice in PBS tween 20 for 2 min. Then they were blocked with 5% normal mice serum for 30 min at room temperature. Incubation with the following primary antibodies was performed for 30 min:

1 Proliferating cell nuclear antigen (PCNA): This antigen is a cofactor of DNA polymerase-δ which is essential for DNA replication, DNA repair and chromatin remodeling. It was detected by rabbit polyclonal IgG (FL-261; catalogue number SC-7907, 200 μg/ml, dilution 1:50, Santa Cruz Biotechnology, USA). Brown discoloration of the nuclei, in the proliferating cells, indicates a positive reaction of nuclear regeneration (Porter 1999).

2 Caspase-3 antibody: Caspase-3 is an essential mediator of programmed cell death; apoptosis. Anti-caspase-3 mouse monoclonal primary antibody (Dako Company, Cairo, Egypt. Catalog No. IMG-144A at a dilution 1/200) was used (Zedan et al., 2015). The slides were rinsed in PBS, incubated with 2 drops of biotinylated secondary antibody for each section for 20 min then rinsed with PBS. Substrate chromagen (DAB) mixture was applied for 5 min then rinsed with distilled water. The slides were stained with hematoxylin then dehydrated and mounted. Brown discoloration of the cytoplasm indicates a positive reaction of the apoptotic cells (Folye et al., 1991).

2.7. Histomorphometric Measurements

Ten non-overlapping fields, randomly chosen, per specimen at a magnification of 400 were examined by an independent observer, using Leica LAS, V3.8 image analyzer computer system (Switzerland). The image analyzer was calibrated automatically to convert the measurement units (pixels) into micrometre units. The area percent of collagen fibers in Masson's trichrome, positive immune reaction for PCNA and caspase-3 stained sections were measured. The area percent represented the areas of the positive reaction, masked by a binary blue color to the area bounded within a standard measuring frame (7286.783 μm^2) and the area percent of stained cells was quantified using Cellsens dimension software (Olympus, Tokyo, Japan) (Liliu et al., 2015).

2.8. Statistical Analysis

All the measurements were expressed as mean and standard deviation (± SD) and subjected to statistical analysis using "SPSS 22" (SPSS, Inc, Chicago, Illinois, USA) software. Analysis of variance using one-way ANOVA and Post-Hoc tests were utilized for comparison between quantitative variables. Results were considered significant when the p-value was less than 0.05 (Armitage, 1994).

 doi:10.20944/preprints202401.1871.v1

3. Results

3.1. Biochemical Results

Regarding the four groups treated with MSCs (groups III-VI), The ALT was significantly decreased in relation to group II (CCl4-treated group). The ALT was significantly increased in the two groups treated with CCl4 and BM-MSCs (group III) and CCl4 and AD-MSCs (group V) compared with the control and the MT-treated MSCs groups (groups IV and VI). Better results were revealed in groups IV and VI with no significant increase of ALT in group VI (CCl4 and MT pre-treated AD-MSCs group) in relation to the control group ($P < 0.05$) (Table 1, Figure 1).

Table 1. Mean values ± standard deviation of the levels of serum enzymes.

Groups	TNF-α	IL-1β	NF-κ β
I	1.06±0.34	0.59±0.24	1.67±0.23
II	465.51±82.54	2.93±0.44	818.03±28.08
III	2.14±0.27[b]	2.70±0.40[a,d,e,f]	301.58±30.09 [a,b,f]
IV	1.80±0.14[b]	1.49±0.58[a,b,c,f]	266.41±45.61 [a,b,f]
V	1.92±0.05[b]	1.91±0.54 [a,b,c,f]	288.90±35.20 [a,b,f]
VI	1.02±0.48[b]	0.36±0.19 [b,c,d,e]	121.92±15.59 [a,b,c,d,e]

[a] statistically significant compared with group I, [b] statistically significant compared with group II,. [c] statistically significant compared with group III, [d] statistically significant compared with group IV,. [e] statistically significant compared with group V, [f] statistically significant compared with group VI,.

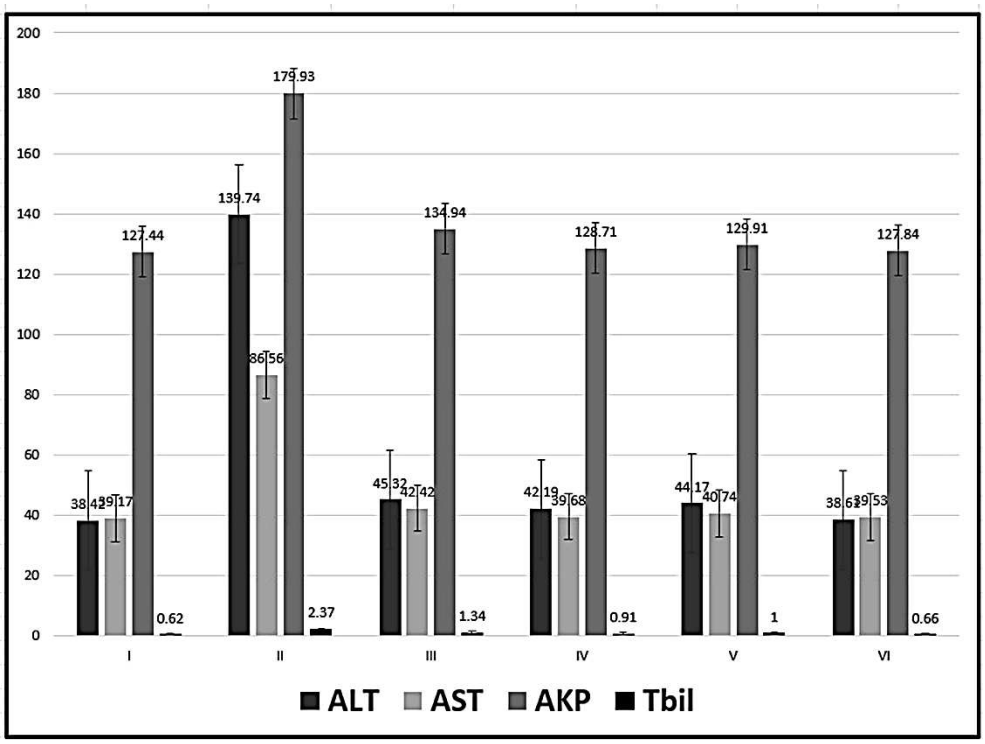

Figure 1. Mean values ± standard deviation of the levels of serum enzymes.

The AST, in the four groups treated with MSCs, was significantly decreased in relation to group II (CCl4-treated group) with no significant difference in relation to the control group and in relation to each other. While the AKP and Tbil were significantly decreased in the four groups treated with MSCs in relation to group II (CCl4-treated group) and in relation to each other except group III (CCl4 and BM-MSCs) ($P < 0.05$) (Table 1, Figure 1).

 doi:10.20944/preprints202401.1871.v1

3.2. Real Time PCR for TNF-α, IL-1ß and NF-κß Gene Expression

Detection of mRNA demonstrated a significant decrease in the expression of TNF-α in in the four groups treated with MSCs (groups III-VI) in relation to group II (CCl4-treated group) with no significant difference in relation to the control group and in relation to each other. In addition, the level of IL-1ß was significantly decreased in the groups treated with MSCs (except group III) in relation to group II (CCl4-treated group) and significantly increased in relation to the control group except for group VI (CCl4 and MT pre-treated AD-MSCs group). the level of NF-κß was significantly decreased in the groups treated with MSCs in relation to group II (CCl4-treated group) and significantly increased in relation to the control group with a significant decrease in group VI (CCl4 and MT pre-treated AD-MSCs group) in relation to the other three groups treated with MSCs ($P < 0.05$) (Table 2, Figure 2).

Table 2. Mean values ± standard deviation of gene expression of TNF-α, IL-1β and NF-κ β.

Groups	TNF-α	IL-1β	NF-κ β
I	1.06±0.34	0.59±0.24	1.67±0.23
II	465.51±82.54	2.93±0.44	818.03±28.08
III	2.14±0.27[b]	2.70±0.40[a,d,e,f]	301.58±30.09 [a,b,f]
IV	1.80±0.14[b]	1.49±0.58[a,b,c,f]	266.41±45.61 [a,b,f]
V	1.92±0.05[b]	1.91±0.54 [a,b,c,f]	288.90±35.20 [a,b,f]
VI	1.02±0.48[b]	0.36±0.19 [b,c,d,e]	121.92±15.59 [a,b,c,d,e]

[a] statistically significant compared with group I, [b] statistically significant compared with group II, [c] statistically significant compared with group III, [d] statistically significant compared with group IV, [e] statistically significant compared with group V, [f] statistically significant compared with group VI,.

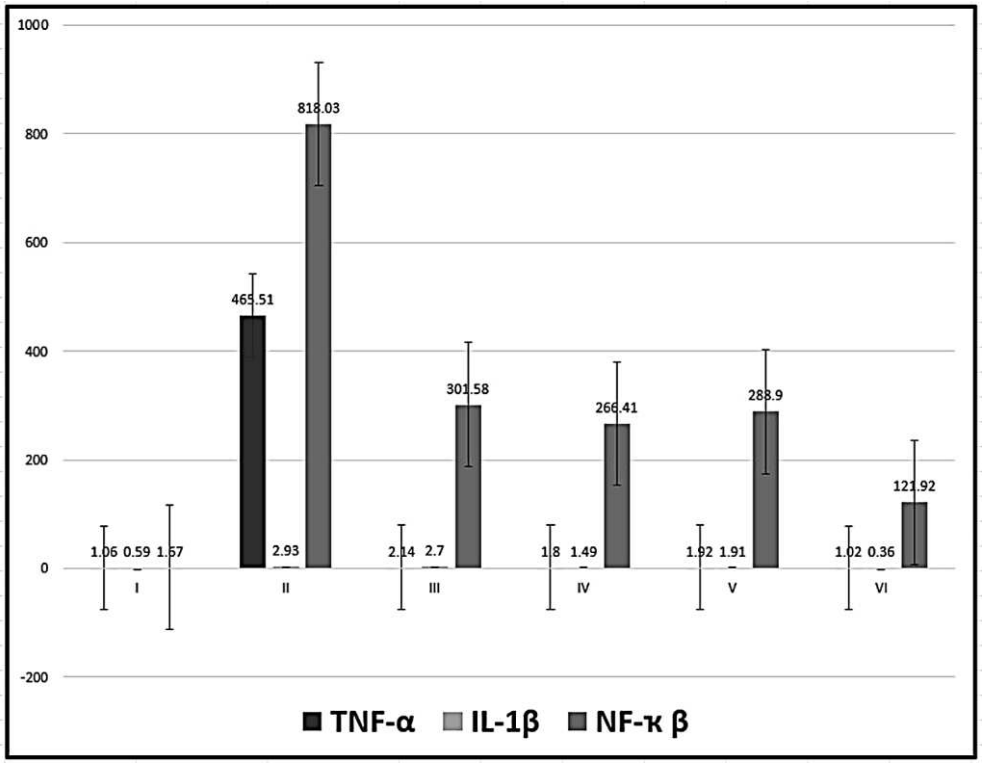

Figure 2. Mean values ± standard deviation of gene expression of TNF-α, IL-1β and NF-κ β.

3.3. Haematoxylin and Eosin Stain

Examination of the control group (group I) specimens showed the normal architecture of the liver tissue around the central vein and the portal triad. The central veins were surrounded by

 doi:10.20944/preprints202401.1871.v1

radiated cords of hepatocytes and hepatic sinusoids with Kupffer cells attached to the endothelium of sinusoids without any pathological changes. The nuclei appeared vesicular with prominent nucleoli and some binucleated cells were detected (Figure 3A–C). The CCl4-treated group (group II) revealed degeneration of the hepatocytes with loss of their normal laminar pattern. Necrosis in the form of nuclear karyolysis and karyorrhexis was seen with the dissolution of the cytoplasm and vacuolar degeneration of the hepatocytes. Inflammatory cellular infiltration, sinusoidal congestion, dilated and congested portal vein with portal edema, periportal fibroplasia, and hemosiderosis with bile duct dilatation and hyperplasia, were observed (Figures 3D–F and 4A). Group III (CCl4 and BM-MSCs treated group) showed moderate vacuolar degeneration of the hepatocytes and bile duct dilatation and hyperplasia with minimal inflammatory cellular infiltration (Figure 4B,C). Group IV (CCl4 and MT pre-treated BM-MSCs group) shows apparently normal hepatocytes with minimal periportal inflammatory cellular infiltration (Figure 4 D). Group V (CCl4 and AD-MSCs treated group) shows minimal bile duct dilatation and hyperplasia, minimal inflammatory cellular infiltration and periportal leukocytic infiltration (Figure 4E,F). Group VI (CCl4 and MT pre-treated AD-MSCs group) shows apparently normal hepatocytes and Kupffer cells (Figure 4G,H).

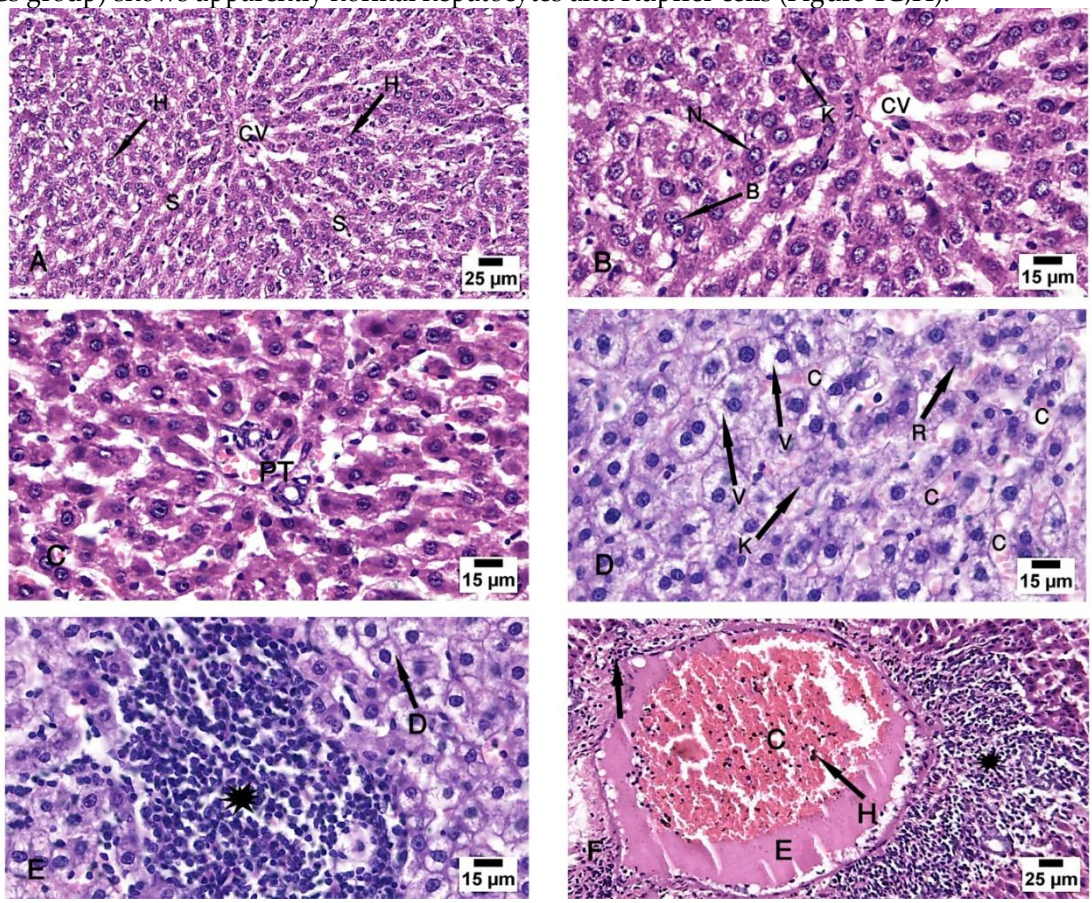

Figure 3. Photomicrographs of the liver tissue (**A–C**) Group I shows the normal architecture of the liver tissue around the central vein (CV) and the portal triad (PT). The central vein is surrounded by radiated cords of hepatocytes (H) and hepatic sinusoids (S). The Kupffer cells (K) are seen attached to the endothelium of sinusoids. The nuclei appeared vesicular with prominent nucleoli (N) and some binucleated cells are noted (B). (**D–F**) Group II shows degeneration of the hepatocytes with loss of their normal laminar pattern. Necrosis in the form of nuclear karyolysis (K) and karyorrhexis (R) with sinusoidal congestion (C) and vacuolar degeneration of hepatocytes (V) are seen. Inflammatory cellular infiltration (asterisk), dissolution of the cytoplasm (D), dilated and congested (C) portal vein with portal edema (E) periportal fibroplasia (arrow) and hemosiderosis (H) are observed. (H & E; A & F x 200, B, C, D & E x 400).

 doi:10.20944/preprints202401.1871.v1

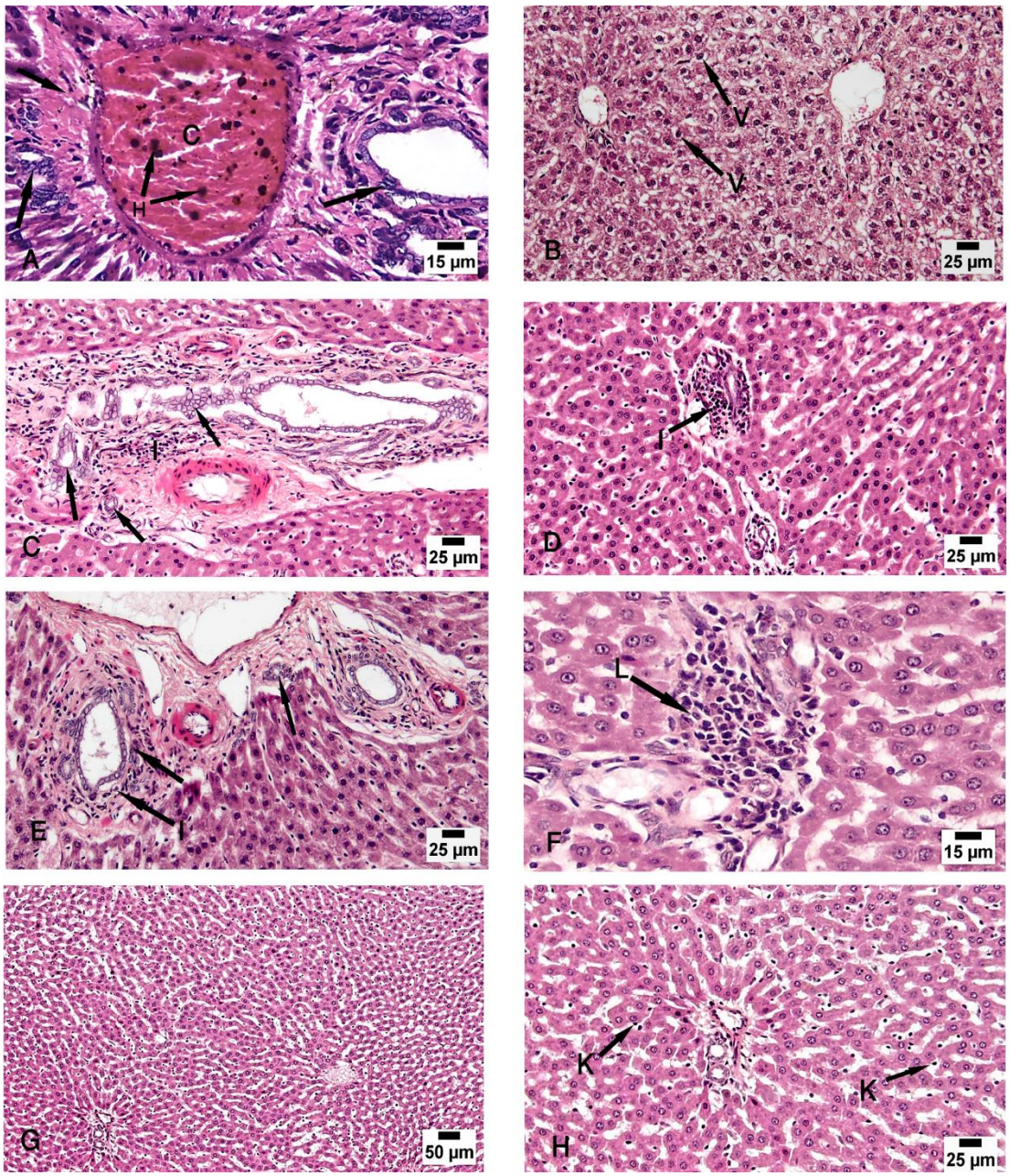

Figure 4. Photomicrographs of the liver tissue (**A**) Group II shows periportal fibroplasia, bile duct dilatation and hyperplasia (arrow) and congested (C) portal vein with hemosiderosis (H). (**B**,**C**) Group III shows moderate vacuolar degeneration of the hepatocytes (V) and bile duct dilatation and hyperplasia (arrow) with minimal inflammatory cellular infiltration (I). (**D**) Group IV shows apparently normal hepatocytes with minimal periportal inflammatory cellular infiltration (I). (**E**,**F**) Group V shows minimal bile duct dilatation and hyperplasia (arrow), minimal inflammatory cellular infiltration (I) and periportal leukocytic infiltration (L). (**G**,**H**) Group VI shows apparently normal hepatocytes and Kupffer cells (K). (H & E; A & F x 200, B, C, D, E & H x 400, G x 100).

3.4. Masson's Trichrome Stain

Specimens of the control group (group I) showed a minimal amount of collagen fibers around the periportal area (Figure 5A,B). Group II (CCl4-treated group) revealed an increased amount of collagen fibers around the periportal area (Figure 5C,D). The specimens of group III (CCl4 and BM-MSCs treated group) showed a moderate amount of collagen fibers around the periportal area (Figure 5E,F). Group IV (CCl4 and MT pre-treated BM-MSCs group) shows a minimal amount of collagen fibers around the periportal area (Figure 6A,B). Group V (CCl4 and AD-MSCs treated group) shows

 doi:10.20944/preprints202401.1871.v1

a moderate amount of collagen fibers around the periportal area (Figure 6C,D). Group VI (CCl4 and MT pre-treated AD-MSCs group) shows a minimal amount of collagen fibers around the periportal area (Figure 6E,F).

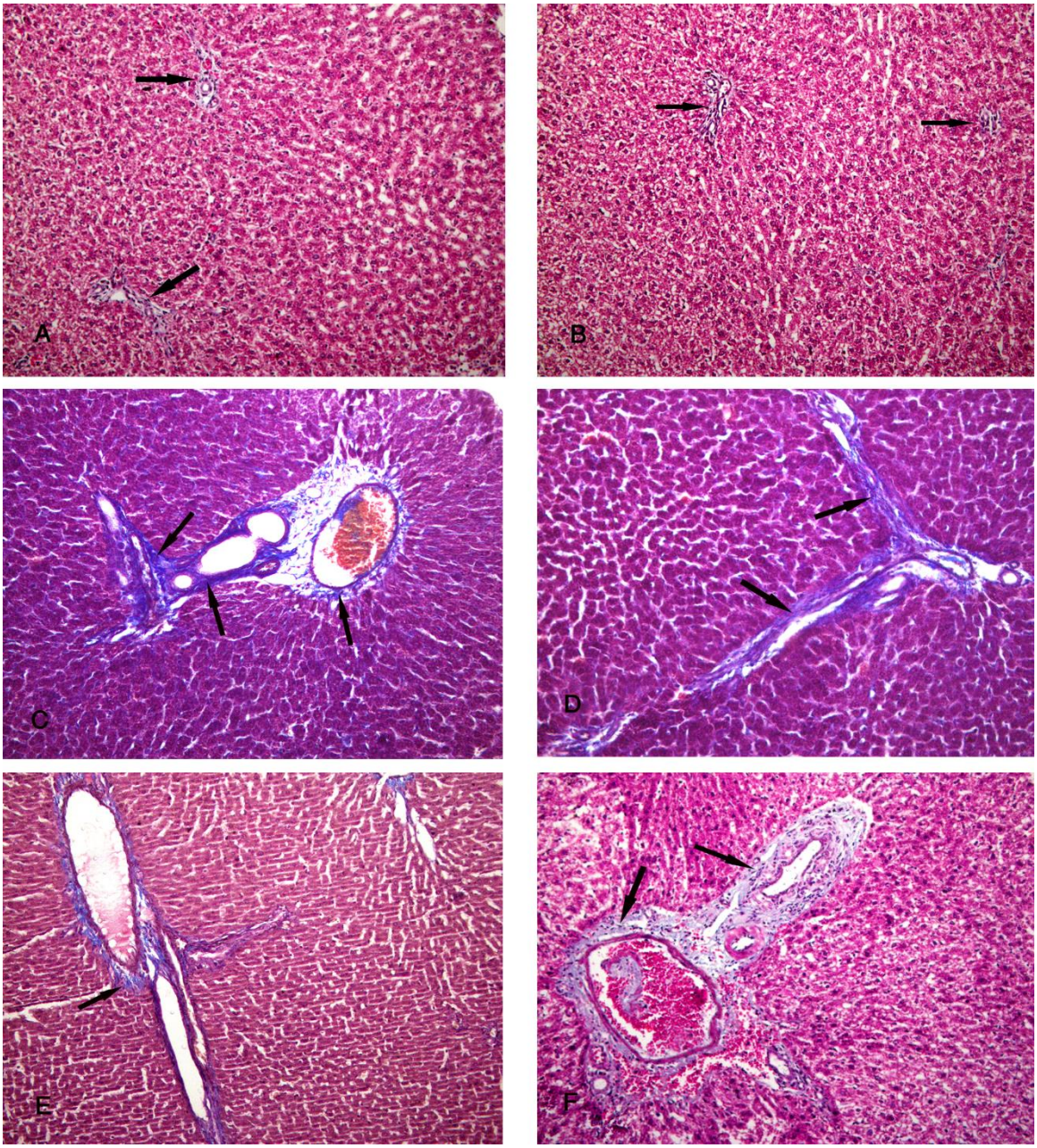

Figure 5. Photomicrographs of the liver tissue (**A**,**B**) Group I shows a minimal amount of collagen fibers around the periportal area (arrows). (**C**,**D**) Group II shows an increased amount of collagen fibers around the periportal area (arrows). (**E**,**F**) Group III shows a moderate amount of collagen fibers around the periportal area (arrows). (Masson's Trichrome x 200).

 doi:10.20944/preprints202401.1871.v1

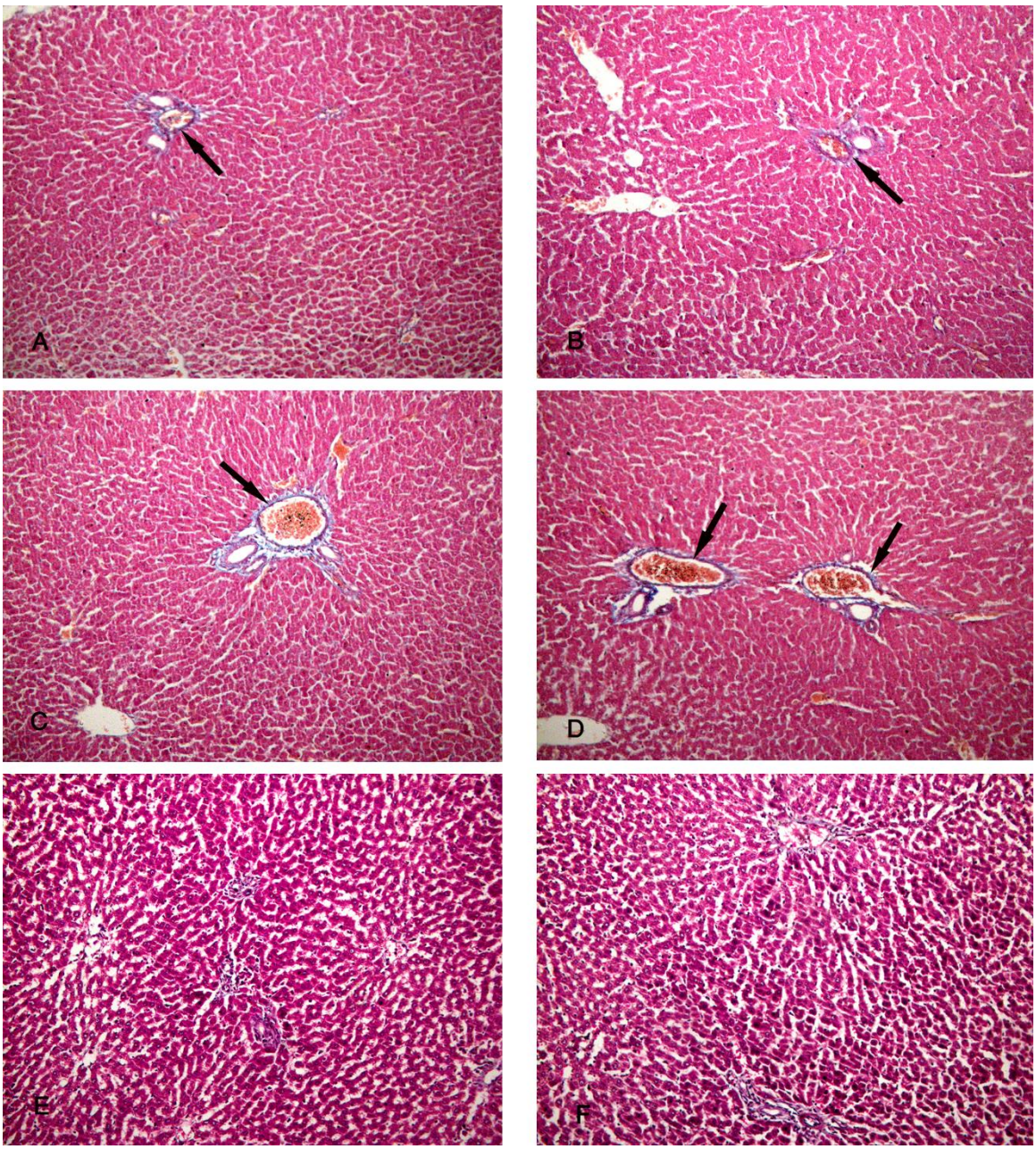

Figure 6. Photomicrographs of the liver tissue (**A**,**B**) Group IV shows a minimal amount of collagen fibers around the periportal area (arrows). (**C**,**D**) Group V shows a moderate amount of collagen fibers around the periportal area (arrows). (**E**,**F**) Group VI shows a minimal amount of collagen fibers around the periportal area (arrows). (Masson's Trichrome x 200).

3.5. PAS Stain

Specimens of the control group (group I) showed normal storage of glycogen in the healthy hepatocytes and a strong reaction of PAS stain (Figure 7A). Group II (CCl4-treated group) showed a marked decrease in PAS-stained hepatic lobules (Figure 7B). Group III (CCl4 and BM-MSCs treated group) showed a decrease in PAS-stained hepatic lobules (Figure 7C). Groups IV (CCl4 and MT pre-treated BM-MSCs group) and V (CCl4 and AD-MSCs treated group) showed an increase in PAS-stained hepatic lobules (Figure 7D,E). Group VI (CCl4 and MT pre-treated AD-MSCs group) showed apparently normal PAS-stained hepatic lobules (Figure 7F).

 doi:10.20944/preprints202401.1871.v1

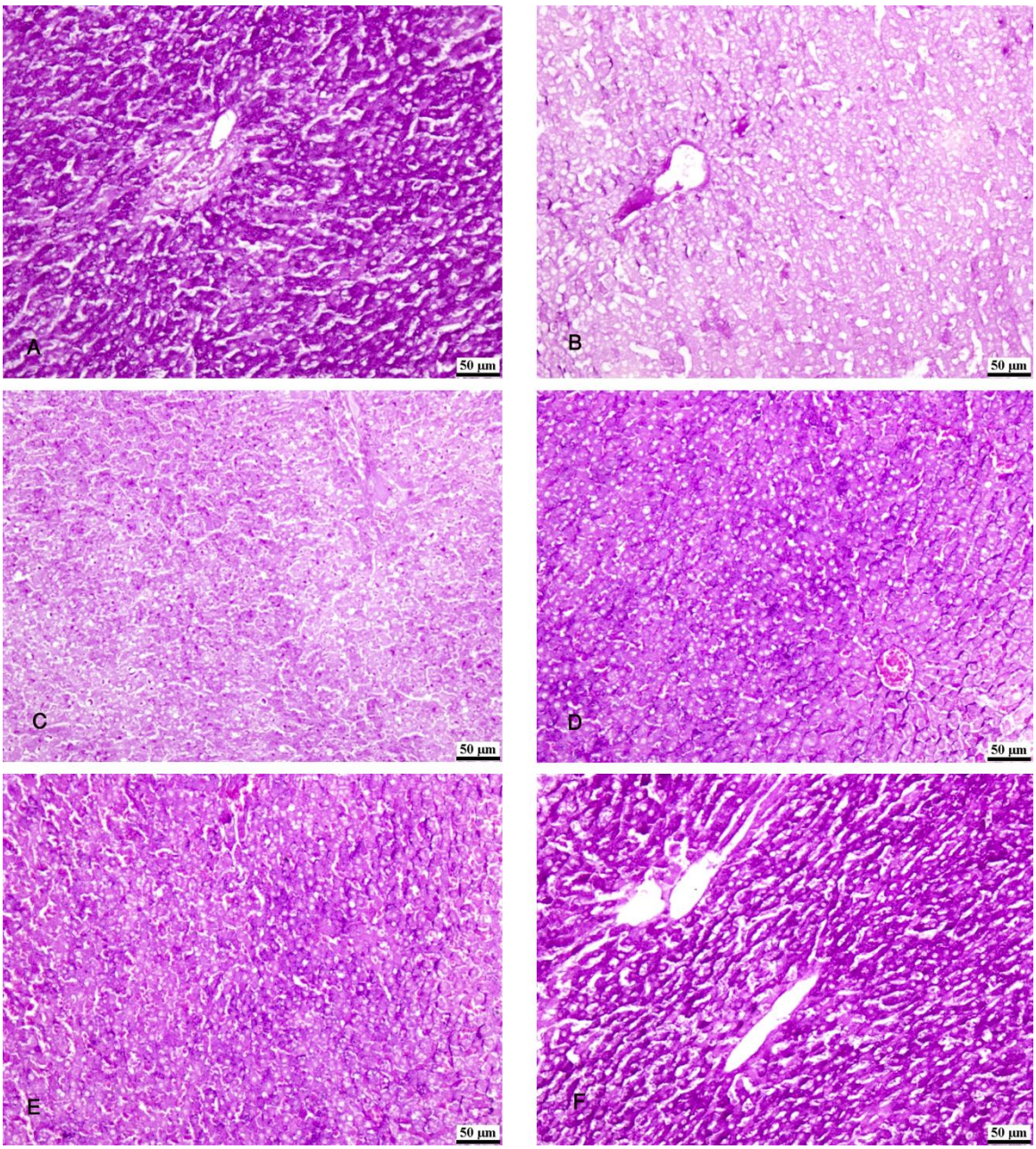

Figure 7. Photomicrographs of the liver tissue (**A**) Group IV shows normal PAS-stained hepatic parenchyma. (**B**) Group II shows a marked decrease in PAS-stained hepatic lobules. (**C**) Group III shows a decrease in PAS-stained hepatic lobules. (**D**,**E**) Groups IV and V show an increase in PAS-stained hepatic lobules. (**F**) Group VI shows apparently normal PAS-stained hepatic lobules. (PAS x 200).

3.6. Immunofluorescent Study for Ki-67

Specimens of the control group showed moderate immunofluorescent yellow-green reaction to the marker indicator of proliferation Ki-67 (Figure 8A), while, the CCl4-treated group (group II) showed minimal yellow-green reaction to Ki-67 (Figure 8B). The specimens of the CCl4 and BM-MSCs treated group and CCl4 and MT pre-treated BM-MSCs group (groups III and IV) revealed moderate immunofluorescent yellow-green reaction to Ki-67 (Figure 8C,D). The specimens of CCl4 and AD-MSCs treated group and CCl4 and MT pre-treated AD-MSCs group (groups V and VI) revealed increased immunofluorescent yellow-green reaction to Ki-67 (Figure 8E,F).

 doi:10.20944/preprints202401.1871.v1

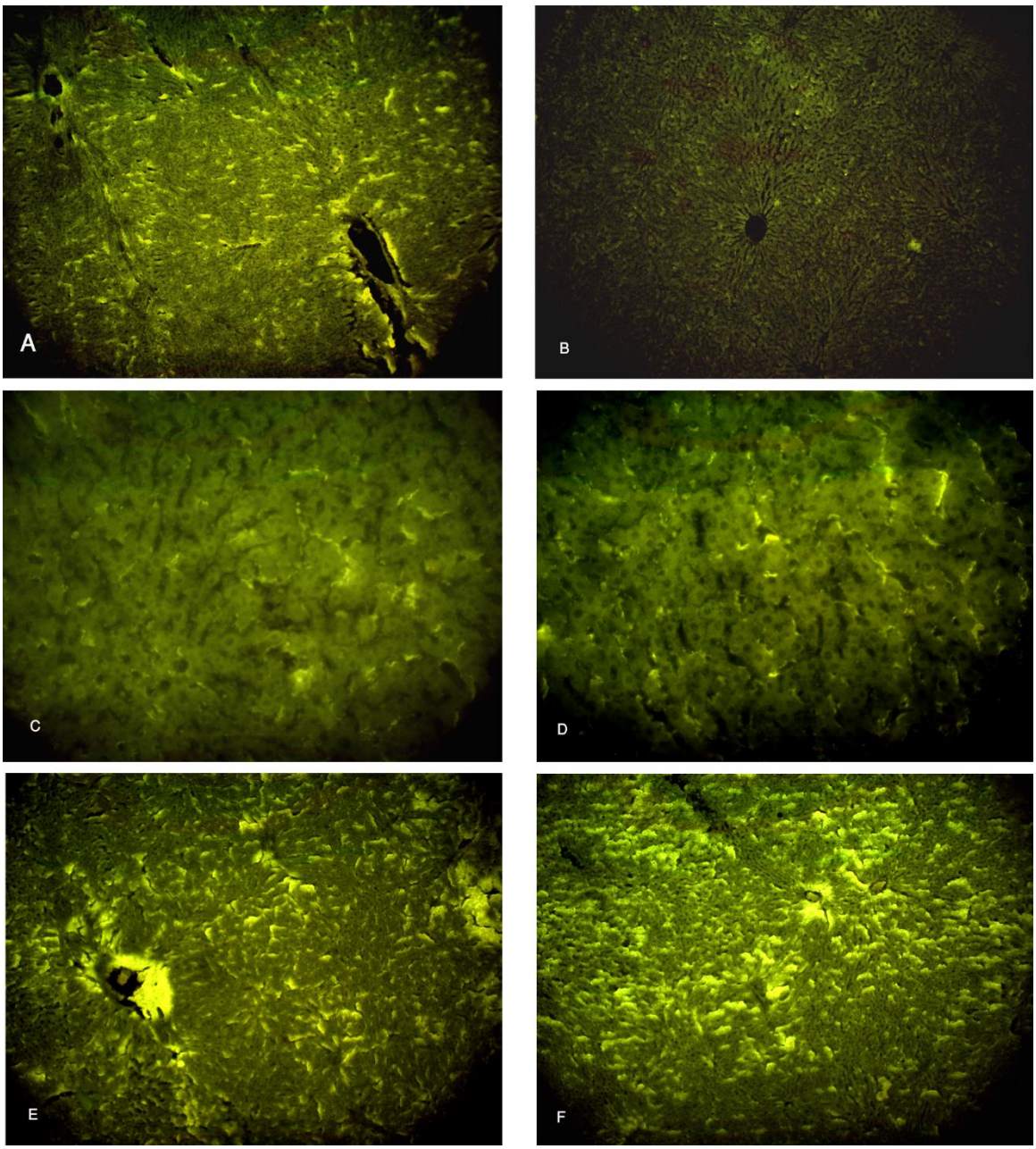

Figure 8. Photomicrographs of the liver tissue (**A**) Group I shows a moderate immunofluorescent yellow-green reaction. (**B**) group II shows a minimal immunofluorescent yellow-green reaction. (**C**,**D**) Groups III & IV show moderate immunofluorescent yellow-green reactions. (**E**,**F**) Groups V & VI show increased immunofluorescent yellow-green reactions. (Ki-67 x 100).

3.7. Immunohistochemical Reaction

The liver specimens of the rats of group I (control group) showed few PCNA reactions in the form of brown nuclei of the hepatocytes. Group II (CCl4-treated group) revealed almost negative PCNA reactions. The liver specimens of group III (CCl4 and BM-MSCs treated group) revealed a moderate number of brown nuclei of the hepatocytes. Groups IV and V (CCl4 and MT pre-treated BM-MSCs group and CCl4 and AD-MSCs treated group) showed an increased number of brown nuclei of the hepatocytes. Almost all the nuclei of the hepatocytes showed brown coloration in group VI (CCl4 and MT pre-treated AD-MSCs group) (Figure 9A–F). Regarding the immune reaction to caspase-3, the hepatocytes of groups I, IV, V and VI showed absence of brown discoloration of the hepatocytes indicating absence of caspase-3 reaction; apoptosis. Group III showed minimal brown

 doi:10.20944/preprints202401.1871.v1

discoloration of the hepatocytes, while group II revealed massive brown discoloration (Figure 10 A–F).

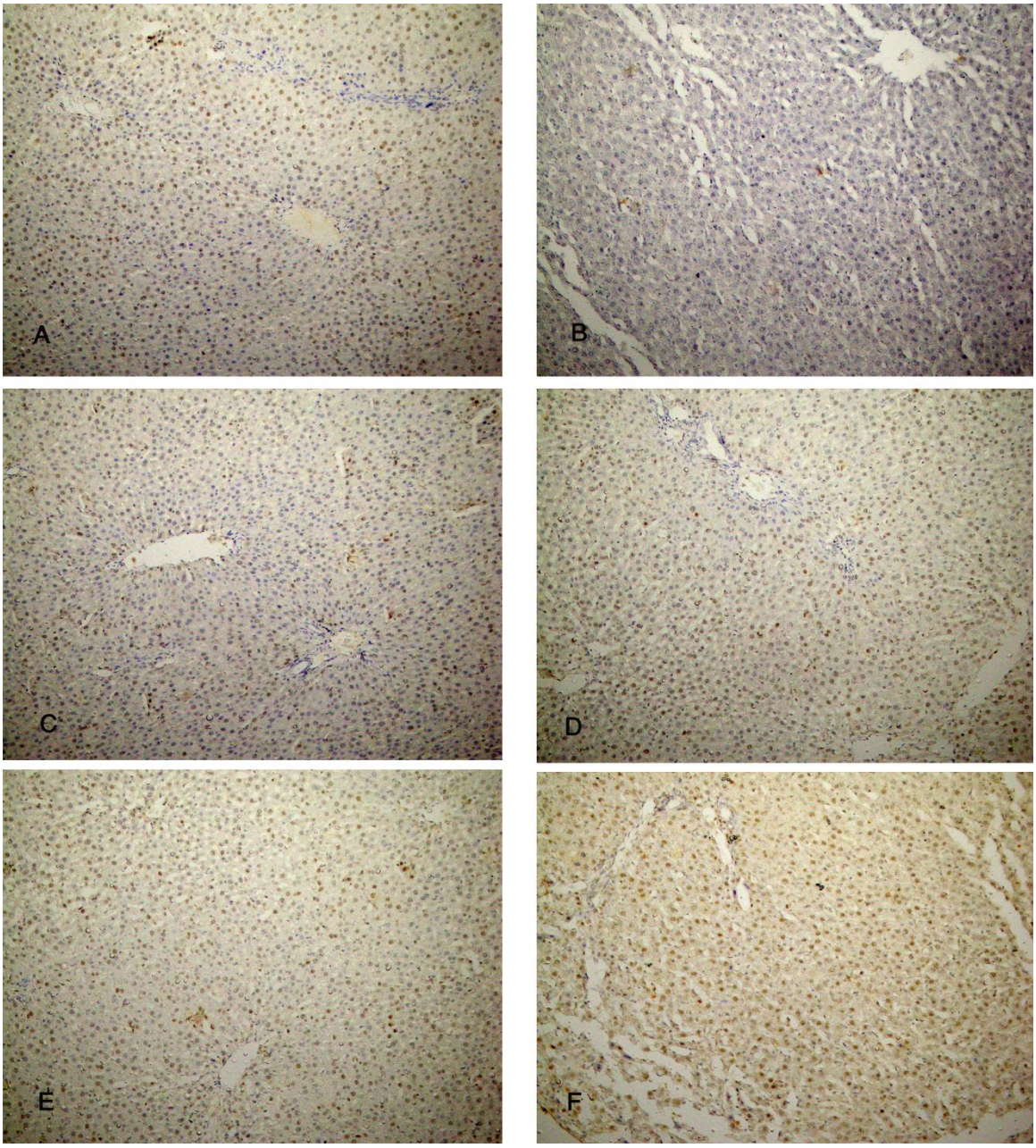

Figure 9. Photomicrographs of the liver tissue (**A**) Group I shows few brown nuclei of hepatocytes. (**B**) Group II shows an almost negative PCNA reaction in the nuclei. (**C**) Group III shows a moderate number of brown nuclei of hepatocytes. (**D**,**E**) Groups IV & V show an increased number of brown nuclei of hepatocytes. (**F**) In Group VI, almost all the nuclei show brown coloration (PCNA x 200).

 doi:10.20944/preprints202401.1871.v1

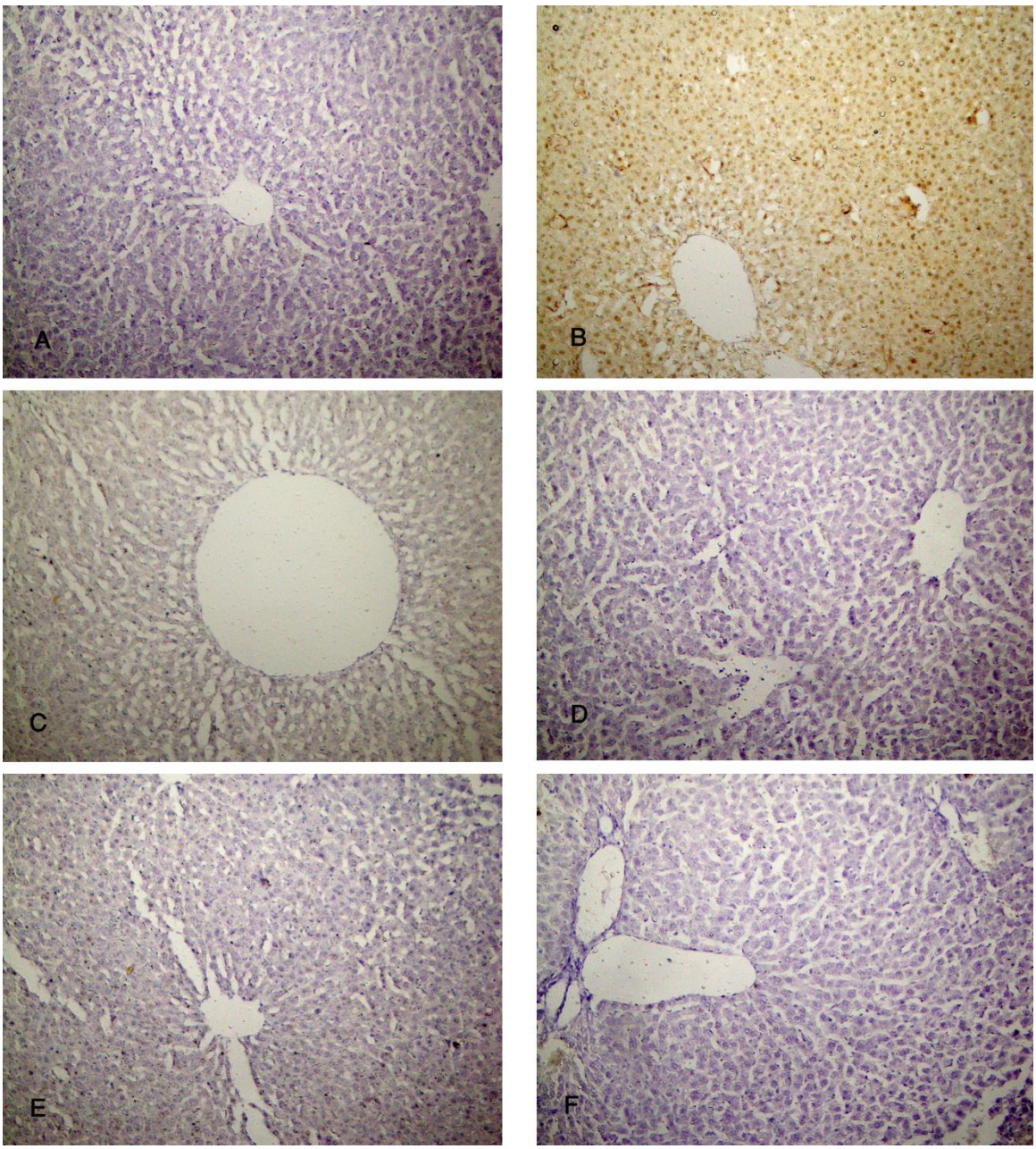

Figure 10. Photomicrographs of the liver tissue (**A**) Group I, (**D**) Group IV, (**E**) Group V and (**F**) Group VI show an absence of brown discoloration of hepatocytes. (**B**) Group II shows massive brown discoloration of hepatocytes. (**C**) Group III shows minimal brown discoloration of hepatocytes. (Caspase-3 x 200).

3.8. Histomorphometric Results

The mean area percent of collagen fibres was significantly decreased in in the four groups treated with MSCs, in relation to group II (CCl4-treated group) while there is no significant difference between the groups treated with MT-treated MSCs (groups IV and VI) and the control group. No statistical difference was observed in the analysis of PAS area percent in group III (CCl4 and BM-MSCs) in relation to group II (CCl4-treated group) with a significant decrease in relation to all other groups. While the best results were revealed in group VI (CCl4 and MT pre-treated AD-MSCs group), where there is no significant difference in relation to the control group and significant increase in relation to all the other groups. The area percent of PCNA reactions, in the four groups treated with MSCs, was significantly increased in relation to group II (CCl4-treated group) and to the control group and in relation to each other. Higher PCNA reaction was revealed in group VI (CCl4 and MT

 doi:10.20944/preprints202401.1871.v1

pre-treated AD-MSCs group). The mean area percent of the immune reaction of caspase-3, in the four groups treated with MSCs, was significantly decreased in relation to group II (CCl4-treated group) with no significant difference in relation to the control group and in relation to each other ($P < 0.05$) (Table 3, Figure 11).

Table 3. Mean values ± standard deviation of the area percent of Masson Trichrome, PAS stains, PCNA and Caspase-3 reactions.

Groups	Masson Trichrome	PAS	PCNA	Caspase-3
I	3.99±0.55	19.50±1.78	8.17±0.75	0.03±0.02
II	17.08±1.89	2.90±0.95	3.02±0.72	59.03±4.28
III	10.95±1.93 ^{a,b,d,f}	3.55±0.91 ^{a,d,e,f}	13.71±3.27 ^{a,b,d,e,f}	0.19±0.25 ^{b}
IV	5.51±0.56 ^{b,c,e}	15.84±1.45 ^{a,b,c,f}	48.42±4.44 ^{a,b,c,f}	0.05±0.04 ^{b}
V	10.11±1.53 ^{a,b,d,f}	15.85±1.53 ^{a,b,c,f}	46.88±4.53 ^{a,b,c,f}	0.05±0.04 ^{b}
VI	4.61±0.72 ^{b,c,e}	18.63±1.34 ^{b,c,d,e}	83.91±6.31 ^{a,b,c,d,e}	0.03±0.02 ^{b}

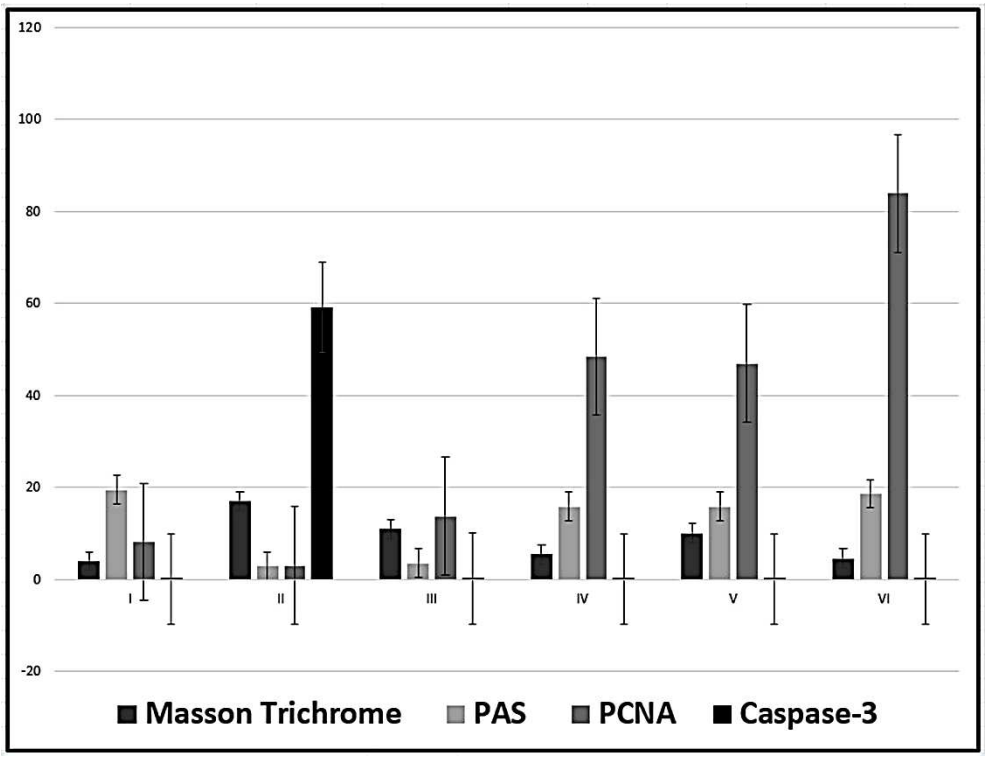

Figure 11. Mean values ± standard deviation of the area percent of Masson Trichrome, PAS stains, PCNA and Caspase-3 reactions.

4. Discussion

Classically when evaluating liver function, the procedures will include measuring the levels of serum alanine aminotransferase (ALT), aspartate aminotransferase (AST), alkaline phosphatase (AKP), and total bilirubin (TBIL) as a term of "liver function tests". However, this term is a misname as many of the elements measured in these tests do not indicate the function of the liver but rather determine the source of the damage. According to Vagvala and O'Connor (2018) and Kwo et al. (2017), hepatocellular injury could be denoted by ALT and AST elevations disproportional to AKP and Tbil. However, elevation of AKP and Tbil out of proportion to ALT and AST indicates obstructive or cholestasis causes. Elevation of all these parameters represents a mixed injury which was determined in the findings of the present study. These results indicate hepatocellular injury denoted by the histopathological alterations in the hepatocytes together with the bile duct dilatation denoting cholestasis and obstructive jaundice in the CCl4 group in agreement with Yacout et al. (2012). The

authors detected elevation of these serum marker enzymes in the rats receiving CCl4 due to liver damage from this hepatotoxic agent. The moderate changes in the groups receiving both BM and AD-MSCs indicate the potential therapeutic effects of MSCs with the best results in group VI (CCl4 and MT-pre-treated AD-MSCs) that appeared almost normal. The levels of ALT, AST, AKP, and TBIL in only group VI had no significant difference compared with the control group indicating that AD-MSCs represent better regenerative effects than BM-MSCs and MT pre-treatment increased their efficacy compared with group V in which AD-MSCs were not pre-treated with MT. In this context, Yilmaz and Karakayali (2023) reported that AD-MSCs achieved better liver function than BM-MSCs in the liver failure model of CCl4. The authors described the main mechanism of improving liver function tests as the ability of AD-MSCs to inhibit hepatocyte degeneration and necrosis with enhancement of their survival rates together with their anti-inflammatory and anti-apoptotic actions.

MSCs modulate liver regeneration through migration, differentiation, hepatocyte regeneration, angiogenesis, and immunoregulation through the activation of multiple proliferative signalling pathways. Concerning migration and differentiation, it has been revealed that MSCs are attracted to the liver by multiple chemotactic signals such as the concentration gradient of stromal cells-derived factor-1 (SDF-1) present in liver sinusoid endothelial cells. SDF-1 enhances the activation of α4β1 integrin of MSCs to firmly adhere to the endothelial cells (Chute, 2006). Chemokine receptor (CXCR7) overexpression, under hypoxic conditions, stimulates the migration of MSCs by increasing the levels of vascular cells adhesion molecule-1 (VCAM-1), and CD 44 (Liu et al., 2018). Hepatic specification of MSCs is induced by fibroblast growth factor 2 (FGF2), fibroblast growth factor 4 (FGF4) and hepatocyte growth factor (HGF) (Snykers et al., 2011). Hepatogenesis of MSCs in the injured liver is triggered through the integrin pathway and downregulation of focal adhesion kinase (FAK) and integrin-linked kinase (ILK) leading to a significant increase of hepatogenic molecules such as HGF, oncostatin M (OSM) and bFGF in MSCs (Bi et al., 2017). MSCs were shown to affect the gene expression of TNF-α, IL-6, HGF, and transforming growth factor-beta (TGF-β) (Abdelhafez et al., 2021) which influence hepatocytes proliferation. The immunomodulation capacity of MSCs is attributed to the intercellular contact and secretion of signaling factors acting on various immune cells. MSCs were shown to inhibit the activation of hepatic stellate cells through the prevention of the proliferation of CD8+ cytotoxic T-lymphocytes and CD4+T-helper (Th) and stimulation of the regulatory T cells through the secretion of TGF-β, prostaglandin E2 (PGE2) and human leukocyte antigen-5 (HLA-G5) (Gazdic et al., 2015; Pianta et al., 2015). MSCs eliminate the profibrotic environment under the effect of IL-4 and IL-10. Phosphorylation of anti-apoptotic hepatic protein kinase (AKT) produces overexpression of IL-10 and TGF-β and reduces the secretion of IL-12 which enhances the differentiation of mature type 1 dendritic cells (DC1s) to the tolerogenic type 2 dendritic cells (DC2s) in the presence of IL-6 and HGF (Li et al., 2021; Hu et al., 2021). MSCs affect the polarization of macrophages decreasing the gene expression of pro-inflammatory mediator TGF-β1 which is considered the chief molecule in the activation of hepatic stellate cells (He et al., 2021) and increase the secretion of milk fat globule-EGF factor 8 (MFGE8) which reduce the TGF-β type I receptor (TGFBR1) (An et al., 2017). Other pro-inflammatory cytokines were reduced such as interferon-γ (IFN-γ), IL-6, IL-1β, IL-12, IL-4 and TNF-α by secreting PGE2, TNF-α stimulated gene/protein 6 (TSG-6), granulocyte-colony stimulating factor (G-CSF) and IL-6. On the other hand, MSCs stimulate the production of anti-inflammatory mediators IL-1, IL-4 and hepatic nuclear factor-4 alpha (HNF-4α) by increasing the nitric oxide synthase (iNOS) through the activation of NF-κB pathway (Ye et al., 2019; Cruz-Barrera et al., 2020). Another effect of the NF-κB pathway is the modulation of hepatic stellate cell proliferation through mediating reactive oxygen species (Roehlen et al., 2020). As shown in the results of the present study, TNF-α, IL-1 β were decreased and NF-κB was elevated in the groups treated with MSCs with the highest expression in the MT pre-treated AD-MSCs. These findings could overcome the limitations of harvesting BM-MSCs such as the limited number obtained, the signs of senescence during expansion and the pain and morbidity as a result of bone marrow aspiration process as reported by Dmitrieva et al. (2012). On the contrary, AD-MSCs could be obtained from multiple sites with minimal invasion and abundant numbers (Farre-Guasch et al., 2010; Iyyanki et al., 2015). Hao et al. (2017) concluded that AD-MSCs significantly reduced the

 doi:10.20944/preprints202401.1871.v1

proliferation and activation of hepatic stellate cells more than the BM-MSCs. In addition, TGF-B1 was secreted in the culture medium of AD-MSCs at significantly higher levels than those of the BM-MSCs. However, the levels of IL-10 and VEGF didn't differ significantly between them. Moreover, the authors denoted that AD-MSCs promoted the anti-inflammatory and anti-fibrotic effects on liver tissue more than BM-MSCs, but still these results were not significant. Although, the present study revealed the same findings but they were statistically significant. In addition, the current work examined the proliferative activity of AD-and BM-MSCs using the immunofluoresent and the immunohistochemistry staining of the proliferative indicators Ki-67 and PCNA, respectively, which revealed increased expression with the group receiving AD-MSCs which was more effective in the MT pretreated group.

MT was demonstrated to produce an antioxidant influence protecting the hepatocytes from free radical injury and inhibiting the pro-inflammatory cytokines such as TNF-α and IL-1β retarding the development of liver fibrosis (Tahan et al., 2009). MT intensely inhibits neutrophil, mononuclear cells, macrophages and mast cells which decrease hepatocyte degeneration and necrosis and produce reduction in the deposition of extracellular matrix (Aktas et al., 2014). Czaja (2014) reported that MT reduced serum transaminase activity and decreased hepatic fibrosis scores as a result of high expression of NF-κB in liver tissue. These finding are in agreement with those of the current study. The groups of MT pre-treated BM- and AD-MSCs revealed better biochemical, histopathological and gene expression results with apparently normal parameters with AD-MSCs treated group. MT was detected to attenuate the expression of apoptotic factor Bax in CCl4-induced hepatic fibrosis (Ogeturk et al., 2008). The pro-inflammatory factors activate antiapoptotic hepatic protein kinase (AKT) phosphorylation that affects the apoptotic gene expression levels of Bax and caspase-3. AKT was proven to play an important role in hepatic stellate cells activation and collagen synthesis stimulating extracellular matrix deposition and promoting liver fibrosis (Peng et al., 2017; Mohammed et al., 2021**)**. Moreover, MT was found to promote the functionality of MSCs improving their therapeutic potential **(**Heo et al., 2019**)**. They added that MT improved the biological activities and proliferation of AD-MSCs in agreement with the results of the current study. These findings were confirmed in the current work as TNF-α, IL-1ß and caspase-3 reactions were reduced in the experimental groups receiving MSCs with the addition that the best results were shown in the MT pre-treated AD and BM-MSCs. Additionally, MT was determined to enhance the self-renewal potential of MSCs, improve their functional activity (Shuai et al., 2016; Li et al., 2019) and inhibit their replicative senescence, especially of AD-MSCs acting as an anti-aging agent (Zhou et al., 2015). In agreement with the current work, the pro-inflammatory cytokines TNF-α, IL-1ß, known to induce cellular senescence (Lin et al., 2009), were reduced in the groups received MT-treated MSCs with the best results in AD-MSCs group.

5. Conclusions

The present study compared the ability of two types of MSCs; AD and BM-MSCs, with and without the pre-treatment of MT, to reduce hepatic fibrosis using CCl4-liver injured rat models. It was observed that both types of MSCs improved the functions of liver cells and reduced the histopathological alterations in the liver tissue. However better results were revealed with AD-MSCs pre-treated with MT. In addition, the immunomodulatory influence of this group showed the best results expressed in the levels of anti-inflammatory, anti-fibrotic, apoptotic and proliferative factors; TNF-α, IL-1β, NF-κB, caspase-3, Ki67 and PCNA. Therefore, it could be included that AD-MSCs when pre-treated with MT represent a very significant tool for future stem cell regenerative and therapeutic strategies for the treatment of liver diseases.

Acknowledgment: The authors gratefully acknowledge the Deanship of Scientific Research, Qassim University for great assistance and funding the publication of this research.

Conflicts of Interest: The authors declare no conflicts of interest.

References

1. Abdelhafez, D., Aboelkomsan, E., El Sadik, A. O. et al. (2021). The Role of Mesenchymal Stem Cells with Ascorbic Acid and N-Acetylcysteine on TNF-α, IL 1β, and NF-$\kappa\beta$ Expressions in Acute Pancreatitis in Albino Rats. *Journal of Diabetes Research*, 6229460, https://doi.org/10.1155/2021/6229460
2. Aktas, C., Kanter, M., Erboga, M., Mete, R. & Oran, M. (2014). Melatonin attenuates oxidative stress, liver damage and hepatocyte apoptosis after bile-duct ligation in rats. *Toxicol Ind Health*, 30:835-844.
3. An, S.Y., Jang, Y.J., Lim, H.J. et al. (2017). Milk fat globule-EGF factor 8, secreted by mesenchymal stem cells, protects against liver fibrosis in mice. *Gastroenterology*, 152,1174–86. https:// doi. org/10. 1053/j. gastro. 2016. 12. 003.
4. Armitage, P. & Berry, G. (1994). Statistical methods in medical research, 3rd ed., Blackwell Scientific Publications, London.
5. Asrani S.K., Devarbhavi H., Eaton J. & Kamath P.S. (2019). Burden of liver diseases in the world. *J Hepatol*, 70(1), 151-171. DOI: 10.1016/j.jhep.2018.09.014
6. Bakker, A.D., Da Silva, V.C., Krishnan, R. et al. (2009). Tumor necrosis factor alpha and interleukin-1beta modulate calcium and nitric oxide signaling in mechanically stimulated osteocytes. *Arthritis Rheum*, 60: 3336-3345, 40.
7. Bancroft, J.D. & Cook, H.C. (1994). Manual of histological techniques and diagnostic applications, 2nd edition. Churchill Livingstone, Edinburgh, London, Madrid, Melbourne, New York, Tokyo.
8. Bi, H., Ming, L., Cheng, R., Luo, H., Zhang, Y. & Jin, Y. (2017). Liver extracellular matrix promotes BM-MSCs hepatic differentiation and reversal of liver fibrosis through activation of integrin pathway. *J Tissue Eng Regen Med*, 11,2685–98. https:// doi. org/ 10. 1002/ term. 2161.
9. Caplan, A.I. (2017). Mesenchymal stem cells: time to change the name! Stem Cells. *Transl Med*, 6,1445–51. https:// doi. org/ 10. 1002/ sctm. 17- 0051
10. Chen, M., Przyborowski, M. & Berthiaume, F. (2009). Stem cells for skin tissue engineering and wound healing. *Crit Rev Biomed Eng*, 37(4–5),399–421.
11. Chu, D.T., Phuong, T.N.T., Tien, N.L.B. et al. (2020). An update on the progress of isolation, culture, storage, and clinical application of human bone marrow mesenchymal stem/stromal cells. *Int J Mol Sci*, https:// doi. org/ 10. 3390/ ijms2 10307 08
12. Chute, J.P. (2006). Stem cell homing. *Curr Opin Hematol*, 1,399–406. https:// doi. org/ 10. 1097/ 01. moh. 00002 45698. 62511. 3d
13. Cruz-Barrera, M., Florez-Zapata, N., Lemus-Diaz, N. et al. (2020). Integrated analysis of transcriptome and secretome from umbilical cord mesenchymal stromal cells reveal new mechanisms for the modulation of inflammation and immune activation. *Front Immunol*, 11,575488. https:// doi. org/ 10. 3389/ fimmu. 2020. 575488.
14. Czaja, A.J. (2014). inflammation and progressive liver fibrosis in chronic liver disease. *World J Gastroenterol*, 20:2515-2532.
15. Dmitrieva, R.I., Minullina, I.R., Bilibina, A.A., Tarasova, O.V., Anisimov, S.V. & Zaritskey, A.Y. (2012). Bone marrow- and subcutaneous adipose tissue-derived mesenchymal stem cells: differences and similarities. *Cell Cycle*, 11: 377-383 DOI: 10.4161/cc.11.2.18858
16. El Aasar, H., Rashed, L., El Sadik A., Amer, R. & Emam, H. (2021). The role of the adipose tissue-derived mesenchymal stem cells enriched with melatonin on pancreatic cellular regeneration. *Folia Morphologica*, #84579 2021 DOI: 10.5603/FM.a2021.0093
17. El Sadik, A., Mohamed, E. & Elzainy, A. (2018). Postnatal changes in the development of rat submandibular glands in offspring of diabetic mothers: Biochemical, histological and ultrastructuralstudy. *PLoS ONE*, 13(10), e0205372. https://doi.org/10.1371/journal.pone.0205372
18. El Sadik, A., El Ghamrawy, T.A. & Abd El-Galil, T.I. (2015). The Effect of Mesenchymal Stem Cells and Chitosan Gel on Full Thickness Skin Wound Healing in Albino Rats: Histological, Immunohistochemical and Fluorescent Study. *PLoS ONE*, 10(9), e0137544. https://doi.org/10.1371/journal.pone.0137544
19. Farre-Guasch, E., Marti-Page, C., Hernadez-Alfaro, F., Klein-Nulend, J. & Casals, N. (2010). Buccal fat pad, an oral access source of human adipose stem cells with potential for osteochondral tissue engineering: an in vitro study. *Tissue Eng Part C Methods*, 16:1083–94.
20. Foley, J.F., Dietrich, D.R., Swenberg, J.A. et al. (1991). Detection and Evaluation of Proliferating Cell Nuclear Antigen (PCNA) in Rat Tissue by an Improved Immunohistochemical Procedure. *J Histotechnol*, 14(4), 237–241.
21. Forman, H.J. (2016). Redox signaling: an evolution from free radicals to aging. *Free Radic Biol Med*, 97,398-407.
22. Gazdic, M., Volarevic, V., Arsenijevic, N. & Stojkovic, M. (2015). Mesenchymal stem cells: a friend or foe in immune-mediated diseases. *Stem Cell Rev Rep*, 11,280–7. https:// doi. org/ 10. 1007/ s12015- 014- 9583-3.
23. Hao, T., Chen, J., Zhi, S., Zhang, Q., Chen, G. & Yu, F. (2017). Comparison of bone marrow-vs. adipose tissue-derived mesenchymal stem cells for attenuating liver fibrosis. *Exp Ther Med*, 14(6):5956-5964. doi: 10.3892/etm.2017.5333.

24. He, Y., Guo, X., Lan, T. et al. (2021). Human umbilical cord-derived mesenchymal stem cells improve the function of liver in rats with acute-on-chronic liver failure via downregulating Notch and Stat1/ Stat3 signaling. *Stem Cell Res Ther*, 12,396. https:// doi. org/ 10.1186/ s13287- 021- 02468-6.
25. Heo, J.S., Pyo, S., Lim, J., et al. (2019). Biological effects of melatonin on human adipose-derived mesenchymal stem cells. *International Journal of Molecular Medicine*, 44, 2234-2244. https://doi.org/10.3892/ijmm.2019.4356
26. Hu, C., Wu, Z. & Li, L. (2020). Mesenchymal stromal cells promote liver regeneration through regulation of immune cells. *Int J Biol Sci*, 16,893–903. https:// doi. org/ 10. 7150/ ijbs. 39725.
27. Hu, C., Zhao, L., Tao, J. & Li, L. (2019). Protective role of melatonin in early-stage and end-stage liver Cirrhosis. *J Cell Mol Med*, 23,7151–7162. DOI: 10.1111/jcmm.14634
28. Hu, J., Chen, X., Li, P. et al. (2021). Exosomes derived from human amniotic fluid mesenchymal stem cells alleviate cardiac fibrosis via enhancing angiogenesis in vivo and in vitro. *Cardiovasc Diagn Ther*, 11,348–61. https:// doi. org/ 10. 21037/ cdt- 20- 1032.
29. Huang, K.C., Chuang, M.H., Lin, Z.S. et al. (2019). Transplantation with GXHPC1 for liver cirrhosis: phase 1 trial. *Cell Transplant*, 28,100S-111S. https:// doi. org/ 10. 1177/ 09636 89719 884885
30. Iyyanki, T., Hubenak, J., Liu, J., Chang, E.I., Beahm, E.K. & Zhang, Q. (2015). Harvesting technique affects adipose-derived stem cell yield. *Aesthet Surg J*, 35:467–76.
31. Jang, Y.O., Kim, M.Y., Cho, M.Y., Baik, S.K., Cho, Y.Z. & Kwon, S.O. (2014). Effect of bone marrow-derived mesenchymal stem cells on hepatic fibrosis in a thioacetamide-induced cirrhotic rat model. *BMC Gastroenterol*, 14:198.
32. Kao, Y.H., Lin, Y.C, Lee, P.H. et al. (2020). Infusion of human mesenchymal stem cells improves regenerative niche in thioacetamide-injured mouse liver. *Tissue engineering and regenerative medicine*, 17,671–82. https:// doi. org/ 10. 1007/ s13770- 020- 00274-4
33. Karsdal, M.A., Krarup, H., Sand, J.M. et al. (2014). Review article: the efficacy of biomarkers in chronic fibroproliferative diseases - early diagnosis and prognosis, with liver fibrosis as an exemplar. *Aliment Pharmacol Ther*, 40, 233-249 DOI: 10.1111/apt.12820
34. Kisseleva, T. & Brenner, D. (2021). Molecular and cellular mechanisms of liver fibrosis and its regression. *Nat Rev Gastroenterol Hepatol*, 18(3),151–66.https:// doi. org/ 10. 1038/ s41575- 020- 00372-7
35. Kwo, P.Y., Cohen, S.M. & Lim, J.K. (2017). ACG Clinical Guideline: Evaluation of Abnormal Liver Chemistries. *Am J Gastroenterol*, 112(1):18-35.
36. Li, H., Zhang, Y., Liu, S. *et al*. (2019). Melatonin enhances proliferation and modulates differentiation of neural stem cells via autophagy in hyperglycemia. *Stem Cells*, 37: 504-515.
37. Li, Y.H., Shen, S., Shao, T. et al. (2021). Mesenchymal stem cells attenuate liver fibrosis by targeting Ly6Chi/lo macrophages through activating the cytokine-paracrine and apoptotic pathways. *Cell death discovery*, 7,239. https:// doi. org/ 10. 1038/ s41420- 021- 00584-z.
38. Lilliu, M.A., Solinas, P., Cossu, M, et al. Diabetes causes morphological changes in human submandibular gland: a morphometric study. *J Oral Pathol Med*, 44,291–295.
39. Liu, L., Chen, J.X., Zhang, X.W. et al. (2018). Chemokine receptor 7 overexpression promotes mesenchymal stem cell migration and proliferation via secreting Chemokine ligand 12. *Sci Rep*, 8,204. https:// doi. org/ 10. 1038/ s41598- 017- 18509-1.
40. Liu, P., Mao, Y., Xie, Y., Wei, J. & Yao, J. (2022). Stem cells for treatment of liver fibrosis/ cirrhosis: clinical progress and therapeutic potential. *Stem Cell Research & Therapy*, 13, 356 https://doi.org/10.1186/s13287-022-03041-5
41. Lodder, J., Denaes, T., Chobert, M.N. et al. (2015). Macrophage autophagy protects against liver fibrosis in mice. *Autophagy*, 11,1280–92.
42. Luedde, T. & Schwabe, R.F. (2010). NF-κB in the liver--linking injury, fibrosis and hepatocellular carcinoma. *Nat Rev Gastroenterol Hepatol*, 8(2):108-18. doi: 10.1038/nrgastro.2010.213.
43. Ma, L., Wei, J., Zeng, Y. et al. (2022) Mesenchymal stem cell-originated exosomal circDIDO1 suppresses hepatic stellate cell activation by miR-141-3p/PTEN/AKT pathway in human liver fibrosis. *Drug Delivery*, 29,1, 440-453, DOI: 10.1080/10717544.2022.2030428
44. Masola, V., Carraro, A., Granata, S. et al. (2019). In vitro effects of interleukin (IL)-1 beta inhibition on the epithelial-to-mesenchymal transition (EMT) of renal tubular and hepatic stellate cells. *J Transl Med* ,17, 12 (2019). https://doi.org/10.1186/s12967-019-1770-1
45. Mohammed, R.A., Shawky, H.M., Rashed, L.A. et al. (2021). Combined effect of hydrogen sulfide and mesenchymal stem cells on mitigating liver fibrosis induced by bile duct ligation: Role of anti-inflammatory, anti-oxidant, antiapoptotic, and anti-fibrotic biomarkers. *Iran J Basic Med Sci*, 24,1753-1762. doi: https://dx.doi.org/10.22038/IJBMS.2021.56477.12604
46. Muthu, S., Patil, S.C., Jeyaraman, N. et al. (2023). Comparative effectiveness of adipose-derived mesenchymal stromal cells in the management of knee osteoarthritis: A meta-analysis. *World J Orthop*, 14(1): 23-41. DOI: 10.5312/wjo.v14.i1.23

47. Ode, A., Kopf, J., Kurtz, A. et al. (2011). CD73 and CD29 concurrently mediate the mechanically induced decrease of migratory capacity of mesenchymal stromal cells. *Eur Cell Mater*, 6, 26–42.
48. Ogeturk, M., Kus, I., Pekmez, H., Yekeler, H., Sahin, S. & Sarsilmaz, M. (2008). Inhibition of carbon tetrachloride-mediated apoptosis and oxidative stress by melatonin in experimental liver fibrosis. *Toxicol Ind Health*, 24:201-208.
49. Parola, M. & Pinzani, M. (2018). Liver fibrosis: pathophysiology, pathogenetic targets and clinical issues. *Mol Aspects Med*, 65,37–55. https:// doi. org/ 10. 1016/j. mam. 2018. 09. 002.
50. Pelekanos, R.A., Sardesai, V.S., Futrega, K., Lott, W.B., Kuhn, M. & Doran, M.R. (2016). Isolation and expansion of mesenchymal stem/stromal cells derived from human placenta tissue. *J Vis Exp JoVE*, https:// doi. org/ 10. 3791/54204
51. Pellicoro, A., Ramachandran, P., Iredale, J.P. & Fallowfield, J.A. (2014). Liver fibrosis and repair: immune regulation of wound healing in a solid organ. *Nat Rev Immunol*, 14,181-194.
52. Peng, R., Wang, S., Wang, R., Wang, Y., Wu, Y. & Yuan, Y. Antifibrotic effects of tanshinol in experimental hepatic fibrosis by targeting PI3K/AKT/mTOR/p70S6K1 signaling pathways. *Discov Med*, 23,81-94.
53. Petrasek, J., Bala, S., Csak, T. et al. (2012). IL-1 receptor antagonist ameliorates inflammasome-dependent alcoholic steatohepatitis in mice. *J Clin Invest*, 122(10):3476–89.
54. Pianta, S., Bonassi Signoroni, P., Muradore, I. et al. (2015). Amniotic membrane mesenchymal cells-derived factors skew T cell polarization toward Treg and downregulate Th1 and Th17 cells subsets. *Stem Cell Rev Rep*, 11,394–407. https:// doi. org/ 10. 1007/ s12015- 014- 9558-4.
55. Porter, A.G. & Janicke, R.U. (1999). Emerging roles of caspase-3 in apoptosis. *Cell Death Differ*, 6, 99–104.
56. Pradere, J.P., Kluwe, J., De Minicis, S. et al. (2013). Hepatic macrophages but not dendritic cells contribute to liver fibrosis by promoting the survival of activated hepatic stellate cells in mice. *Hepatology*, 58(4):1461–73.
57. Roehlen, N., Crouchet, E. & Baumert, T.F. (2020). Liver fibrosis: mechanistic concepts and therapeutic perspectives. *Cells*, https:// doi. org/ 10. 3390/ cells 90408 75.
58. Sepanlou, S.G., Safiri, S., Bisignano, C. et al. (2020). The global, regional, and national burden of cirrhosis by cause in 195 countries and territories, 1990–2017: a systematic analysis for the Global Burden of Disease Study 2017. *Lancet Gastroenterol Hepatol*, 5, 245–66. https:// doi. org/ 10. 1016/ S2468- 1253(19) 30349-8
59. Shi, M., Li, Y.Y., Xu, R.N. et al. (2021). Mesenchymal stem cell therapy in decompensated liver cirrhosis: a long-term follow up analysis of the randomized controlled clinical trial. *Hepatol Int*, 15,1431–41. https:// doi. org/ 10. 1007/ s12072- 021- 10199-2
60. Shuai, Y., Liao, L., Su, X. et al. (2016). Melatonin Treatment Improves Mesenchymal Stem Cells Therapy by Preserving Stemness during Long-term In Vitro Expansion. *Theranostics*, 6(11),1899–1917.
61. Snykers, S., de Kock, J., Tamara, V. & Rogiers, V. (2011). Hepatic differentiation of mesenchymal stem cells: in vitro strategies. *Methods Mol Biol*, 698,305–14. https:// doi. org/ 10. 1007/ 978-1- 60761- 999-4_ 23.
62. Suk, K.T. & Kim, D.J. (2015). Staging of liver fibrosis or cirrhosis: The role of hepatic venous pressure gradient measurement. *World J Hepatol*, 7(3), 607-615 DOI: 10.4254/wjh.v7.i3.607
63. Tahan, V., Atug, O., Akin, H. et al. (2009). Melatonin ameliorates methionineand choline-deficient diet-induced nonalcoholic steatohepatitis in rats. *J Pineal Res*, 46,401-407.
64. Tsuji, W., Rubin, J.P. & Marra, K.G. (2014). Adipose-derived stem cells: Implications in tissue regeneration. *World J Stem Cells*, 6,312-321. DOI: 10.4252/wjsc.v6.i3.312
65. Vagvala, S.H. & O'Connor, S.D. (2018). Imaging of abnormal liver function tests. *Clin Liver Dis*, 11(5),128-134.
66. Varkouhi, A.K., He, X., Teixeira Monteiro, A.P. et al. (2021). Immunophenotypic characterization and therapeutics effects of human bone marrow- and umbilical cord-derived mesenchymal stromal cells in an experimental model of sepsis. *Exp Cell Res*, 399,112473. https:// doi. org/ 10. 1016/j. yexcr. 2021. 112473.
67. Wagner, G.P., Kin, K. & Lynch, V.J. (2012). Measurement of mRNA abundance using RNA-seq data: RPKM measure is inconsistent among samples. *Theory Biosci*, 131,281–285.
68. Wei, Y.H., Jun, L. & Qiang, C.J. (2004). Effect of losartan, an angiotension II antagonist, on hepatic fibrosis induced by CCl4 in rats. *Dig Dis Sci*, 49,1589-1594.
69. Xie, Y., Liu, S., Wang, L. et al. (2021). Individual heterogeneity screened umbilical cord-derived mesenchymal stromal cells with high Treg promotion demonstrate improved recovery of mouse liver fibrosis. *Stem Cell Res Ther*. 12,359. https:// doi. org/ 10. 1186/s13287- 021- 02430-6
70. Yang, Y.M.& Seki, E. (2015). TNFα in liver fibrosis. *Curr Pathobiol Rep*, 3(4),253-261. doi: 10.1007/s40139-015-0093-z.
71. Ye, Z., Lu, W., Liang, L. et al. (2019). Mesenchymal stem cells overexpressing hepatocyte nuclear factor-4 alpha alleviate liver injury by modulating anti-inflammatory functions in mice. *Stem Cell Res Ther*, 10,149. https:// doi. org/ 10. 1186/ s13287- 019- 1260-7.
72. Yilmaz, T.U. & Karakayali, L. (2023). The versatility of adipose derived stem cells in liver transplantation: a narrative review. *Digestive Medicine Research*, doi: 10.21037/dmr-22-24

73. Zedan, W., Mourad, M.I. & Abd El-Aziz, S.M. (2015). Evaluation of Caspase 3 as a Target for Apoptosis induced via Chemotherapy in Rats. *Int J Curr Adv Res*, 3(9),1591–1601.
74. Zhang, J.J., Meng, X., Li, Y. et al. (2017). Effects of melatonin on liver injuries and diseases. *Int J Mol Sci*, 18:2017.
75. Zhang, Y., Li, Y., Zhang, L., Li, J. & Zhu, C. Mesenchymal stem cells: potential application for the treatment of hepatic cirrhosis. *Stem Cell Res Ther*, 9(1),59. https:// doi. org/ 10. 1186/ s13287- 018- 0814-4
76. Zhou, L., Chen, X., Liu, T. et al. (2015). Melatonin reverses H_2O_2-induced premature senescence in mesenchymal stem cells via the SIRT1-dependent pathway. *J Pineal Res*, 59,190–205.
77. Zhou, Q., Rong, C., Gu, T. et al. (2022). Mesenchymal stem cells improve liver fibrosis and protect hepatocytes by promoting microRNA-148a-5p-mediated inhibition of Notch signaling pathway. *Stem Cell Research & Therapy*, 13,354 https://doi.org/10.1186/s13287-022-03030-8
78. Zhou, W., Nelson, E.D., Abu Rmilah, A.A., Amiot, B.P. & Nyberg, S.L. (2019). Stem cellrelated studies and stem cell-based therapies in liver diseases. *Cell Transplant*, 28,1116–22. https:// doi. org/ 10. 1177/ 09636 89719859262